3-16-2023

Time series analysis of *Pseudo-nitzschia* species composition, domoic acid, and environmental conditions in the Gulf of Maine from 2013-2020

Christina Chadwick
University of South Florida

Time series analysis of *Pseudo-nitzschia* species composition, domoic acid, and environmental conditions in the Gulf of Maine from 2013-2020

by

Christina Chadwick

A thesis submitted in partial fulfillment
of the requirements for the degree of
Master of Science
College of Marine Science
University of South Florida

Co-Major Professor: Mya Breitbart, Ph.D.
Co-Major Professor: Katherine Hubbard, Ph.D.
Gary Mitchum, Ph.D.

Date of approval:
March 15th, 2023

Keywords: Species assemblages, DNA fingerprinting, ARISA, toxin

DEDICATION

To my family: mom, dad, Noni, Catherine, Matthew, Julia, and Sean. Without your love and support, I would not be the person I am today. I thank each one of you for pushing me to work my hardest but to also enjoy every moment of life, as tomorrow is never guaranteed. This thesis is especially dedicated to my brother, Stephen, whose love and passion for the ocean inspired me to learn more about this beautifully complex underwater world.

ACKNOWLEDGMENTS

This research was funded by grants from the Woods Hole Oceanographic Institution's NSF/NIEHS Oceans and Human Health program (COHH 2 and 3). I would like to thank my co-advisor and mentor, Dr. Kate Hubbard, for allowing me to grow and develop a career in her lab and for her guidance, patience, and continuous support over the years. Special thank you to my co-advisor, Dr. Mya Breitbart, for her guidance, encouragement, and never-ending positivity. I would also like to thank my committee member, Dr. Gary Mitchum, for his guidance and helpful advice regarding this thesis.

Thank you to Jane Disney, Anna Farrell, Alexis Garretson, Nathan Dorn and the volunteers at Mount Desert Island Biological Laboratory for their sample collection, data entry, and sample processing. Thank you to Yizhen Li for providing the code for calculating upwelling indices and thank you to Eric Mulbach for assistance with visualization. I would also like to thank Matt Garrett for his help with designing the site map for this thesis.

A special thank you to my amazing Florida Fish and Wildlife Research Institute molecular ecology, toxin, and microscopy lab colleagues: Alex DeSmidt, April Granholm, Camden Conte, Cary Lopez, Celia Villac, Emily Denny, Halle Berger, Josee Bouchard, Karen Henschen, Laura Markley, Leanne Flewelling, Leo Eguia, Lydia Ruggles, Maya Robert, Molly Joseph, Stephanie Keller Abbe, Sugandha Shankar, and Taylor Wood for their help with sample processing and data visualizations. I am extremely grateful to learn from and work alongside such incredible scientists.

TABLE OF CONTENTS

LIST OF TABLES

LIST OF FIGURES

ABSTRACT

Phytoplankton are abundant in both fresh and marine waters and can form harmful algal blooms (HABs) by producing potent toxins that have devastating effects on human, wildlife, and economic health. The HAB-forming diatom genus, *Pseudo-nitzschia,* occurs globally and approximately half of the 59 currently identified species can produce the neurotoxin, domoic acid (DA). DA accumulates in shellfish and finfish and can cause Amnesic Shellfish Poisoning (ASP) in humans and DA Poisoning (DAP) in several species of wildlife, resulting in severe neurological dysfunction and mortality. Along with these health threats, DA toxicity is a major economic threat for shellfish and fish farms and toxic *Pseudo-nitzschia* blooms have caused multi-million dollar losses in revenue in several regions due to the closures of seafood farms as a result of high DA levels. DA production varies across *Pseudo-nitzschia* species and strains therefore species identification and continuous monitoring are critical. The Gulf of Maine is an area with emerging DA issues. In 2016, the Gulf of Maine experienced its first shellfishery closure due to ASP in eastern Maine, coincident with the first observance of *Pseudo-nitzschia australis* in this region. Repeated shellfish closures due to *P. australis* presence occurred in 2017, 2018, and 2019. This thesis highlights temporal patterns of *Pseudo-nitzschia* species composition, environmental, hydrodynamic, and nutrient conditions in the Gulf of Maine, which provides potential mechanisms through which these changes are linked to DA production in this region. Findings from this research will enhance early detection capabilities of toxic *Pseudo-nitzschia* species, thus improving monitoring strategies for this HAB-forming genus.

CHAPTER ONE:

INTRODUCTION

Phytoplankton are microscopic plant-like organisms that are abundant in both fresh and marine waters. These diverse organisms play a key role in supporting their surrounding ecosystems by forming the base of the marine food web. Phytoplankton play a major role in oxygenating Earth by consuming carbon dioxide and releasing oxygen through photosynthesis. Estimates suggest approximately 40% of the Earth's carbon is fixed by oceanic phytoplankton (Berger et al., 1989; Martin et al., 1992; Falkowski, 1994). While these microorganisms are essential for marine life, some can form harmful algal blooms (HABs) and produce potent toxins that can have devastating effects on human, wildlife, and economic health. HABs have expanded to affect virtually all coastal countries and their impacts have increased in frequency and intensity over the past several decades (Gobler, 2020) with both natural and anthropogenic explanations proposed for this observed increase (Anderson, 2009). A potential cause for the observed increase in HABs includes dispersal of species via changes in physical forcing such as currents and storms (Anderson, 2009) due to altered oceanic circulation, wind, and precipitation patterns, sea surface temperature, and coastal upwelling events as a result of climate change (Sarkar, 2018). Increasing HABs may also be due to anthropogenic contributions such as phytoplankton cells being transported via ship ballast tank water or sediment (Hallegraeff et al., 1988; Hallegraeff et al., 1990; Hallegraeff and Gollasch, 2006; Anderson, 2009) and increasing industrial, agricultural, and sewage runoff which inevitably enriches coastal waters with excess

nutrients (Anderson, 2009). These anthropogenic inputs have altered the oceanic nutrient regime, creating a more optimal environment for certain HAB species (Anderson, 2009). Understanding the interactions among physical, nutrient, and species dynamics is thus critical for examining the underlying drivers that may be important for changes in HAB distributions.

Pseudo-nitzschia and impacts of domoic acid

Diatoms are a type of eukaryotic phytoplankton that have cell walls composed of silica, referred to as frustules, and are often a dominant component of spring and fall phytoplankton assemblages (Sommer, 1989; Orsini et al., 2004). *Pseudo-nitzschia* is a HAB-forming pennate diatom genus that has been observed globally in estuarine, coastal, and offshore waters. There are currently 59 species of *Pseudo-nitzschia* that have been taxonomically classified (Lelong et al., 2012; 52 species described in Bates et al., 2018; 7 species described in: Ajani et al., 2018; Huang et al., 2019; Dong et al., 2020; Chen et al., 2021; Percopo et al., 2022) and approximately half of these species produce a potent neurotoxin, domoic acid (DA) (Bates et al., 2018) which binds to the N-methyl-D-aspartate receptors in the neurons of the hippocampus (Garcia-Corona et al., 2022). Accumulation of DA in the tissues of filter-feeding shellfish such as clams, mussels, and scallops and can cause Amnesic Shellfish Poisoning (ASP) in humans upon consumption. In the first 24 hours after consuming DA-contaminated seafood, symptoms of ASP include abdominal cramps, nausea, diarrhea, and vomiting (Wright et al., 1989). Neurological issues such as disorientation, difficulty breathing, permanent memory loss, and coma can occur within 48 hours after consumption (Wright et al., 1989; Teitelbaum et al., 1990; reviewed by Lelong et al., 2012) and can lead to death (Perl et al., 1990). In 1987, DA-contaminated mussels

harvested from Prince Edwards Island River estuary in Canada were identified as the cause of an ASP outbreak in humans (Bates et al., 1989). This event resulted in over 100 documented cases of ASP where at least 3 people died within 24 days after consumption (Wright, 1989; Ramsdell and Gulland, 2014). Others experienced seizures, severe impairment of short-term memory, and altered neurological metabolic function (Teitelbaum et al, 1990; Ramsdell and Gulland, 2014). In the most severe cases, patients with ASP were reported to have significant memory loss 5 years after the outbreak (Todd, 1992). The producer of DA during this 1987 event was originally identified as the pennate diatom *Nitzschia pungens* forma *multiseries* (Hasle, 1965), then later classified as *Pseudo-nitzschia multiseries* (Hasle et al., 1996). There have been no human deaths reported since this 1987 incident due to an increase in worldwide monitoring of *Pseudo-nitzschia* cellular abundance in seawater and of DA levels in seawater and shellfish and finfish tissues (Bates et al., 2018).

Domoic acid can also cause DA Poisoning (DAP) in several species of wildlife such as fish, birds, and mammals, resulting in severe neurological dysfunction and mortality (Fritz et al., 1992; Work et al., 1993; Lefebvre et al., 1999; Scholin et al., 2000; Lefebvre et al., 2002). During toxic events, DA accumulation in lower trophic levels, such as zooplankton and planktivorous fish, can lead to widespread transfer of toxicity through marine food webs (Bargu et al., 2002; Trainer et al, 2012). In 1991, high levels of DA produced by *Pseudo-nitzschia australis* caused the deaths of pelicans and cormorants in Monterey Bay, California where high levels of DA were detected in their stomach contents (Fritz et al., 1992; Villac et al., 1993; Work et al., 1993). Later in 1998, over 400 sea lions died in California and many others were reported as suffering neurological issues concurrent with a bloom of *P. australis* and high levels of DA toxicity (Lefebvre et al., 1999; Scholin et al, 2000). At the peak of the bloom, anchovy stomach

contents contained significant levels of DA and high numbers of *P. australis* frustules (Lefebvre et al., 1999; Scholin et al., 2000). In the sea lions, DA and *P. australis* frustules were detected in urine and fecal samples, thus providing evidence of the trophic transfer of this toxin (Lefebvre et al., 1999; Scholin et al., 2000). Another event in Monterey Bay, California in 2000 showed evidence that DA toxicity was transferred to humpback and blue whales via planktivorous fish such as krill, anchovies, and sardines (Lefebvre et al., 2002). Similar to the 1998 event, fragmented *P. australis* frustules and DA were detected in whale fecal samples, suggesting that the source of the frustules was from the ingested prey and not directly from the surrounding water (Lefebvre et al., 2002). Trophic transfer of DA toxicity has also been observed in the Gulf of Maine (GOM) where North Atlantic right whales were likely exposed to DA by ingesting copepod vectors over a period of several months (Leandro et al., 2010).

Along with human and wildlife health impacts, DA toxicity is a major economic threat for shellfish and fish farms. For example, in spring 2015, the U.S. West Coast experienced the most widespread, destructive, and toxic *P. australis* bloom on record and caused a $97.5 million loss in revenue due to the unprecedented closure of the Dungeness crab fishery in Oregon as a result of high DA levels (Du et al., 2016; Moore et al., 2019). Another highly toxic *Pseudo-nitzschia* bloom occurred in the GOM in 2016 and coincided with the first observance of *P. australis* in this region (Bates et al., 2018). During this bloom, shellfish tissue samples exceeded the regulatory threshold limit of 20 µg DA g^{-1} shellfish tissue and samples reached 100 µg DA g^{-1} tissue resulting in this region's first shellfishery closure (Lewis et al., 2017). These unprecedented levels of DA caused several shellfish growing areas to close in Maine and in areas on both sides of the Bay of Fundy, Canada where DA levels were 30 µg DA g^{-1} tissue (Bates et al., 2018). Although DA remained below the regulatory limit in Massachusetts and Rhode Island,

precautionary closures were enforced due to high *Pseudo-nitzschia* cell counts and the proximity of the major toxicity recorded in Maine (Bates et al., 2018). In 2017, high DA levels resulted in shellfish growing area closures in Rhode Island in spring, and again in Maine during late summer/fall, which resulted in another recall of mussels (Bates et al., 2018). In both closures, *P. australis* was again observed and implicated as the species responsible for the high DA levels in this region (Hubbard et al., 2017; Bates et al., 2018). Following these events, repeated closures occurred in Maine in the fall of 2018 and 2019 (Clark et al., 2021) which provides evidence of the emerging issue of DA-related events in this region (Sterling et al., 2022).

Species identification

All *Pseudo-nitzschia* cells have a silica frustule cell wall composed of two valves that fit together (Lelong et al., 2012). Along each valve is a slit referred to as a raphe which has silica bridges, referred to as fibulae, that reinforce the inside of the cell (Amato et al., 2007; Trainer et al., 2008; Lelong et al., 2012). Some species have a central interspace, separated by striae and within the striae are poroids which are tiny holes or perforations that connect the interior of the cell with the exterior medium (Lelong et al., 2012). Each *Pseudo-nitzschia* species has varying spacing and number of fibulae, striae, and poroids which can be seen using electron microscopy (EM) (Hernández-Becerril, 1998; Lundholm et al., 2002; Kaczmarska et al., 2005; Amato et al., 2007). Most species of *Pseudo-nitzschia* have the ability to form chains that vary in length depending on the species (Kaczmarska et al., 2005) or the health of the species. EM is a common way for differentiating *Pseudo-nitzschia* species as opposed to light microscopy, where distinctions at the species level cannot be made. While EM is excellent and necessary for

Pseudo-nitzschia taxonomy, environmental factors, such as growth temperature, have been shown to affect cell morphology in several species. For example, *P. multiseries* grown at different temperatures have differences in numbers of poroid rows (Lewis et al., 1993). Further, pseudo-cryptic and cryptic species diversity has been widely observed within *Pseudo-nitzschia*, such that genetic approaches have provided a complementary taxonomic tool (Lundholm et al., 2003; Orsini et al., 2004; Hasle and Lundholm, 2005; Fernandes et al., 2014).

Sensitive molecular biology approaches for *Pseudo-nitzschia* species identification have been developed that provide additional confirmation and resolution. One method includes targeting and sequencing the large-subunit ribosomal RNA (LSU rRNA) gene to develop species-specific probes (Scholin et al., 1994; Miller and Scholin 1996); however, the lack of polymorphic sites in the LSU (Bornet et al., 2005) made it challenging for downstream methods, such as Fluorescent In Situ Hybridization, Sandwich Hybridization Assays, to specifically target individual species (Miller and Scholin, 1996; Parsons et al., 1999). A DNA fingerprinting method using polymerase chain reaction (PCR) was developed by Bornet et al. (2005) where highly polymorphic markers were designed to identify several species in the *Pseudo-nitzschia* genus. Another widely used DNA fingerprinting method, Automated Ribosomal Intergenic Spacer Analysis (ARISA), was applied to the *Pseudo-nitzschia* genus through the development of genus-specific PCR primers that target a polymorphic region of the internal transcribed spacer 1 (ITS1) (Hubbard et al., 2008, 2014; Marchetti et al., 2008). The ITS1 region is situated between the 18S and 5.8S rRNA genes and varies in length among *Pseudo-nitzschia* species, allowing for differentiation of species based on previously validated sequences. This semi-quantitative and community-based approach approximates the relative abundance of ITS1 copies

from each amplified species rather than providing cellular abundance quantification (Hubbard et al., 2014; Bates et al., 2018).

Drivers and variability in DA production

Toxin production varies in severity across species and across environmental conditions, making identification and monitoring of these toxic and non-toxic species critical. Presence of a toxic *Pseudo-nitzschia* species does not necessarily mean that the toxic species is always producing DA. Past research has shown that not only does a toxic *Pseudo-nitzschia* species need to be present in the system, but that there must also be certain environmental conditions present for the species to produce DA (Lelong et al., 2012). Previous research revealed correlations between environmental drivers, *Pseudo-nitzschia* species, and DA production (Anderson et al., 2006; MacIntyre et al., 2011; Trainer et al., 2012; McCabe et al., 2016; Clark et al., 2019; Bates et al., 2018) but the biological, chemical, and physical drivers that affect DA production are extremely complex and difficult to define. It is thought that there is not one central condition that causes a *Pseudo-nitzschia* species to produce toxin, but rather a combination of several conditions. Toxin production varies by orders of magnitude between species as well as between different strains of the same species (Bates et al., 1998) and differs regionally (Trainer et al., 2012; Fernandes et al., 2014). Studies have shown that toxin production may also be strain-specific, and that this variability could be influenced by several factors such as timing of sexual reproductive cycles and physiological factors characteristic of distinct isolates (Trainer et al., 2012). Previous studies have shown that DA production also varies across the different stages of cell growth. For example, DA production from *P. seriata* isolates from the GOM increased by an

order of magnitude from exponential to early stationary phase and sustained high levels of DA through late stationary phase (Fernandes et al., 2014).

Nutrients

Past studies show that DA production in *P. australis, P. multistriata, P. seriata,* and *P. multiseries* is stimulated under silicate and phosphate limitation and suppressed under nitrate limitation (Bates et al., 1991). Silicate availability has been shown to regulate gene expression in diatoms where certain proteins are formed only in the absence of silicate (Sullivan and Volcani, 1981). Therefore, silicate limitation in the system may favor expression of genes involved in DA biosynthesis (Pan et al., 1998). Silicate availability also regulates the growth and frustule formation of diatom cells (Pan et al., 1996a). Limitation of silicate in the system has been shown to cease cell division, likely due to the termination of DNA synthesis from interruption of the normal cell cycle (Darley and Volcani 1969; Sullivan and Volcani, 1973; Pan et al., 1996a) which causes DA accumulation in the cells (Sauvey et al., 2023). Past research has shown that this decrease in cellular growth resulted in an extended stationary phase, an event that has been connected to higher levels of DA production (Bates et al., 1991; Pan et al., 1996a). In a physiology experiment, *P. multiseries* culture produced DA at two stages; the first stage was caused by low levels of silicate in the growth medium resulting in decreased cell growth rate (Pan et al., 1996a) and the second, which produced DA at an order of magnitude higher than the first stage, was caused by severe silicate depletion (Pan et al., 1996a). This study concluded that cellular DA content greatly depends on cell growth rates (Pan et al., 1996a).

Similar observations were made with phosphate limitation in which DA production increased as the growth rate of *P. multiseries* decreased (Pan et al., 1996b). This study also found

that high rates of DA production and low rates of nutrient uptake coincided with high levels of adenosine triphosphate (ATP) (Pan et al., 1996b), the compound responsible for providing energy to cells. These elevated levels of ATP concurrent with high levels of DA production suggests that there is a high energy requirement for *Pseudo-nitzschia* cells to produce DA (Pan et al., 1996b). In this study, DA concentrations increased within the cells and extracellularly in the medium and authors suggested that this may be due to malformations of the cell membrane due to lack of sufficient phosphorus to build the lipid bilayer (Pan et al., 1996b).

In contrast to silicate and phosphate, nitrate is an essential nutrient for DA biosynthesis and deprivation of this nutrient has been shown to cause cessation of DA production in cultures of *Nitzschia pungens* f. *multiseries* (Bates et al., 1991). In the same experiment, once nitrate was added back into the medium, cells resumed production of DA (Bates et al., 1991). The form of nitrogen may greatly affect toxin production. When in the form of ammonium, high concentrations inhibit growth and higher DA production is supported compared to the same concentration of nitrate (Bates et al., 1993). This observed increase in DA was proposed to be due to arrested cell growth resulting from ammonium toxicity (Bates et al., 1993; Hillebrand and Sommer, 1996). An alternative explanation was that ammonium is energetically favorable for biosynthesis of DA because nitrate is more energetically expensive since it involves enzymes and sequential electron transfers to be reduced to ammonium (Pan et al., 1998). Other factors, such as light levels, may alter the nitrogen preference. Past laboratory studies have shown that *P. cuspidata* grown at low light and fed nitrate were significantly more toxic than cells grown in ammonium or urea (Auro and Cochlan, 2013). While it has been confirmed that nitrogen source plays a role in DA production, species vary in their nutrient responses and therefore a generalization can’t be made to fit all species (Trainer et al. 2012). Similar to nitrate, iron

limitation also plays a critical role in DA production because without iron, chlorophyll synthesis and nitrogen metabolism cannot occur, both of which are required for DA production (Bates et al., 2001).

Changes in nutrient concentrations and therefore nutrient ratios are key drivers of species assemblage shifts (Parsons et al., 2002; Lundholm, 2010; Thorel, 2017). Past growth experiments have shown that *Pseudo-nitzschia* cells dominated over other diatoms in low silicate:nitrate nutrient supply ratio (Sommer, 1994) potentially due to *Pseudo-nitzschia* cells having lightly silicified frustules (Marchetti et al., 2004). There is evidence that nutrient ratios are important in governing toxin production (Anderson et al., 1990; Bates et al., 1991). Specifically, anomalously low silicate:nitrate ratios may act as a physiological stressor that promotes higher cellular DA due to silicate depletion before nitrate. During the 2015 U.S. West Coast *P. australis* bloom previously mentioned, silicate concentrations were anomalously low compared to nitrate, causing silicate to become depleted first which promoted populations with higher cellular DA (Ryan et al., 2017). Low residual silicic acid was also detected in the vastly toxic *P. australis* bloom in the GOM in 2016 (Clark et al., 2019).

Light, temperature, and salinity

Pseudo-nitzschia species can grow in a broad range of temperatures. In laboratory studies, *P. australis* optimal growth temperature is around 13-15 °C (Clark et al., 2021) but has been observed in warm water masses ranging from 12-18 °C (McCabe et al., 2016) on the west coast of the USA and in colder water masses ranging from 1.6-15.4 °C on the east coast of the USA (Roche et al., 2022). Another toxic species, *Pseudo-nitzschia seriata* can grow in temperatures ranging from 4-15 °C (Fehling et al., 2004; Hansen et al., 2011) but morphological

deformities, such as poroid density and number of poroid rows, were observed with increased temperature (Hansen et al., 2011).

Physiology studies have shown the importance of light and temperature for DA production and that toxin production by *P. australis* was elevated with increased temperature (Thorel et al., 2014; Zhu et al., 2017) and light (Thorel et al., 2014). Irradiance has been shown to affect DA production in *P. multiseries* cultures where cellular DA increased with higher temperatures and higher irradiance level of 180 µmol photons m^{-2} s^{-1} compared to lower temperatures and lower irradiance level of 80 µmol photons m^{-2} s^{-1} (Lewis et al., 1993). This drastic increase in temperature and light may have caused physiologically stressful conditions resulting in higher DA production (Bates, 1998). Photoperiod can influence DA production, cell yield, and growth rate and may also influence which *Pseudo-nitzschia* species will dominate an assemblage (Fehling et al., 2005). In Fehling's study, *P. seriata* cultures grown under a longer photoperiod (18 hours light : 6 hours dark) produced more DA than those grown with shorter duration of light (9 hours light : 15 hours dark). However, under the longer photoperiod condition, the proportional increase in cell density was greater than the increase in DA, resulting in a lower DA concentration per cell (Fehling et al., 2005).

Pseudo-nitzschia species have a wide range of salinity tolerances as revealed by past laboratory studies (Thessen, 2005). In Louisiana coastal waters, *Pseudo-nitzschia* has been observed in salinities ranging from 1 to >35 psu but were more prevalent and preferred higher salinities in both field and laboratory observations (Thessen, 2005). Past research has shown that temperature and salinity tolerances of *Pseudo-nitzschia* are dependent on each other. When grown at higher temperatures, *P. cuspidata* was shown to tolerate a wider range of salinities

(Doan-Nhu et al., 2008). Similarly, when *P. cuspidata* was grown with optimal salinity of 30 psu, this species was able to grow at a wider range of temperatures (Doan-Nhu et al., 2008). Similar results were reported for *P. pseudodelicatissima* where cells were able to grow at 5 °C and 25 °C when grown at optimum salinity of 25 psu (Lundholm et al., 1997). When grown at optimum salinity, the lower temperature limit for growth was lower than any other salinity tested (Lundholm et al., 1997) which was consistent with findings on *P. americana* (Miller and Kamykowski, 1986). Experiments studying salinity effects on *Pseudo-nitzschia* DA production have shown conflicting results across different species and strains. While elevated cellular growth rates of *P. multiseries* cells in culture were observed at 20 psu, production of particulate DA (pDA), the DA measured within phytoplankton cells, was shown to be higher in cultures acclimatized to higher salinities such as 30 and 40 psu compared to lower salinities of 10 and 20 psu (Doucette et al., 2008). The induced stress of the lower salinity may have caused the species to shift its energy towards growing as opposed to processes involved in DA synthesis (Doucette et al., 2008). In contrast, *P. australis* isolates grown in a range of salinities (20-40 psu) were shown to have lower growth rate and higher pDA concentrations at the lowest salinity of 20 psu (Ayache et al., 2020).

Hydrodynamic drivers

Blooms of *Pseudo-nitzschia* can be stimulated by nutrients from upwelling and riverine inputs (Trainer et al., 2012). Strong winds may transport toxic blooms inshore from upwelling zones offshore (Trainer et al., 2000, 2002) or may enable mixing of water masses to transport nutrients to the photic zone in the water column (Lund-Hansen and Vang, 2004; Trainer et al., 2012). Resuspension of sediments during such strong wind events transports nitrogen,

phosphorus, and carbon-rich sediment porewater to the water column (Giffin and Corbett, 2003). A previous study showed that high diatom cell abundance was associated with lower water column silicate concentrations, likely because there was rapid uptake of dissolved silicate at the surface waters from the sediments during periods of vertical mixing (Rothenberger et al., 2009). Further, brief events of upwelling-favorable winds followed by periods of relaxed winds were shown to favor diatom growth (Wilkerson et al., 2006) as increased vertical mixing tends to inhibit some dinoflagellates (Rothenberger et al., 2009). On the west coast of the USA, *Pseudo-nitzschia* blooms have been shown to co-occur with upwelling conditions (Lange et al., 1994; Bates et al., 1998b). The growth response to upwelled nutrients is time-lagged most likely because the cells require some time to respond physiologically to the transformed nutrient field (Kudela et al., 1997). Past time series analyses (2002-2011) have shown that the GOM region experiences a wind directional shift from northwesterly to southwesterly winds in April-May which favors coastal upwelling circulation near the coast (Li et al., 2014).

Unlike upwelling, nutrients from riverine discharges are likely due to anthropogenic nutrient loading from agricultural runoff and sewage (Trainer et al., 2012). Nutrient changes accompanied by riverine input may include increased nitrogen and phosphorus as well as decreased silicate:nitrate, as seen in the Mississippi River (Turner and Rabalais, 1991; Trainer et al., 2012). Such nutrient inputs have been shown to increase cellular abundance of *Pseudo-nitzschia* species in association with increased discharge from the Mississippi River and increased submarine ground discharge of nutrients off the coast of Alabama (Liefer et al., 2009; MacIntyre et al., 2011; Trainer et al., 2012). Sediment cores from the Louisiana coast showed similar results where an increase in *Pseudo-nitzschia* abundance was significantly correlated with increased nitrate fluxes and decreased silicate:nitrate (Parsons et al. 2002). Past research has

shown that nitrogen and phosphorus from riverine input have a synergistic effect on algal productivity (Rudek et al., 1991) and that productivity was significantly greater with increased nitrogen and phosphorus than with nitrogen alone (Rudek et al., 1991). Riverine discharge rates have been shown to influence dominance of certain phytoplankton species (Rothenberger et al. 2009). Diatom taxa dominated in a North Carolina estuary when river discharge rates and nitrate were high, and salinity and silicate were low (Rothenberger et al. 2009).

Results from Li et al.'s time-series study (2014) showed that riverine runoff in the GOM was the greatest in April and May and subsided by June and July. The time series showed interannual variability of coastal salinity due to the amount and timing of peak riverine discharge which altered water stratification earlier in the year than expected (Li et al., 2014). This earlier stratification event may have caused nutrients to be depleted earlier in the year, leading to unfavorable growth conditions for another HAB species, *Alexandrium fundyense* (Li et al., 2014). Therefore, timing of hydrodynamic shifts is an important factor to consider when attempting to tease apart *Pseudo-nitzschia* bloom and DA dynamics.

Species competition and community structure

Environmental changes can affect the competitive balance between phytoplankton species and can result in distinct species assemblages across short distances or rapid temporal changes in assemblages. Past research has illustrated that species have differing competitive abilities and resource utilization strategies which govern species dominance under resource limitations (Grover, 1991; Litchman et al., 2007; Burson et al., 2018). For example, changes in community structure due to increasing nutrient loads have been observed in phytoplankton

communities where species shifted from competing for nutrients to competing for light (Burson et al., 2018). In this experiment, smaller species became dominant in nitrogen, phosphorus, and light limitation treatments, suggesting that having a smaller cell size provides a competitive advantage over larger cells (Burson et al., 2018). This finding is supported by other studies that demonstrated dominance of small cells in nutrient-poor environments and that nutrient loading and cell abundance were positively correlated (Cavender-Bares et al., 2001; Li, 2002; Litchman et al., 2007). For example, small diatom cells were identified as being prevalent in a low turbulence and low nutrient regime; large diatoms were prevalent in a highly turbulent and high nutrient regime in the northwest Atlantic (Li, 2002).

Temporal shifts in *Pseudo-nitzschia* species composition and distribution have been observed in several regions. A study using sediment cores from Denmark spanning a 100-year period showed that toxin-producer *P. multiseries* was the dominant species in Denmark before 1947 then shifted to a *P. pungens* and *P. americana*-dominated assemblage with a decreased abundance of *P. multiseries* after 1958 (Lundholm et al, 2010). This study provided evidence that this species assemblage shift was likely due to a combination of nitrogen loading and increased temperature in the area (Lundholm et al., 2010).

Temperature changes may also affect the competitive balance between *Pseudo-nitzschia* species (Lundholm et al., 2010). For example, another *Pseudo-nitzschia* species composition shift was observed in the Skagerrak where *P. multiseries*, which was the dominant species in the late 1960s and 1970s, declined in abundance in the 1990s whereas *P. pseudodelicatissima* abundance increased (Hasle et al., 1996). During this time, *P. pungens* shifted from being observed mostly in autumn before 1986, to occurring year-round (Hasle et al., 1996). A possible

explanation for this shift is that winters in the 1990s in the Skagerrak were milder, thus favoring *P. pungens* growth over *P. multiseries*, which is capable of growing at lower temperatures (Lewis et al., 1993; Hasle et al., 1996; Lundholm et al., 2010). Temperature may also affect the *Pseudo-nitzschia* species composition in a given environment because different species have been shown to sexually reproduce at different temperatures (Kaczmarska et al., 2008; Quijano-Scheggia et al., 2009). For example, *P. delicatissima* strains mated at 12 °C but did not mate at higher temperatures (Kaczmarska et al., 2008) and therefore, certain species can only mate during certain seasons (Quijano-Scheggia et al., 2009). This may be another factor playing a role in the determination of species presence in the *Pseudo-nitzschia* assemblage. In Rhode Island, shellfish harvest closures due to high DA levels occurred when temperatures were 15-20 °C in October 2016 and 1-5 °C in March 2017 (Sterling et al., 2022) which demonstrates that although temperature is likely a governing force of the seasonality of certain species observance, the species assemblages present under certain temperatures are of more importance for determining DA production potential (Sterling et al., 2022).

Past studies have shown the importance of species composition as an indicator for DA and that distinct changes in species diversity on seasonal time scales may impact the timing and magnitude of DA toxicity (Fernandes et al., 2014). A study using ARISA showed that the relative abundance of DA-producing *Pseudo-nitzschia* species greatly influenced DA concentrations between 2013 and 2014 in southern California (Smith et al., 2018). Concentrations of DA were two orders of magnitude higher in 2013 than in 2014 due to differences in *Pseudo-nitzschia* species assemblages (Smith et al., 2018). The 2013 assemblage was dominated by *P. australis/P seriata*, a species complex that cannot be discriminated based on ARISA fragment size in this region, and the 2014 assemblage contained multiple species with

P. cuspidata and *P. heimii/P.americana,* another species complex that is indistinguishable based on the ARISA fragment size, in the highest proportions (Smith et al., 2018). This study concluded that the 2013 bloom of *P. australis/P. seriata* had a greater potential for toxin production than the 2014 mixed assemblage bloom since this species complex has been shown to produce higher DA concentrations (Trainer et al., 2012; Smith et al., 2018) and because the silicic acid limitation in 2013 likely affected DA production (Bates et al., 1991; Pan et al., 1996a; Smith et al., 2018). Similarly, Clark et al. (2019) showed that increases in pDA were observed with increases of toxin-producing *Pseudo-nitzschia* species in the GOM. Samples with *P. plurisecta*, a species with the ability to produce high amounts of DA, had greater pDA concentrations than those with *P. delicatissima* and *P. seriata* and the greatest pDA peak observed in the sample set was in 2016 due to a dominance of the highly toxic species, *P. australis* (Clark et al., 2019).

Thesis goals

This thesis examines trends in *Pseudo-nitzschia* species composition in field samples collected approximately weekly at two sites on Mount Desert Island (Maine, USA), the Bar Harbor Town Pier and Mount Desert Island Biological Laboratory (MDIBL), from 2013-2020 to identify temporal and ecological patterns. The primary goal of this thesis is to characterize bloom dynamics—with a focus on changes in DA toxicity across weekly, seasonal, to interannual time scales—to understand how changes in species assemblages, environmental, hydrodynamic, and nutrient conditions contribute to DA production. The hypotheses for this research are divided into three parts and are outlined here:

Hypothesis I

Given the emerging threat of *P. australis* and DA production in the GOM, I hypothesize that interannual differences in the severity of DA events from 2013-2020 are linked to species composition. I also expect that variability in nutrient levels and nutrient ratios is important for understanding variability in the timing and magnitude of peak toxicity across years.

Hypothesis II

By examining seasonal shifts in *Pseudo-nitzschia* species assemblages, I expect that certain toxic species are linked to increased DA production in summer and fall, and that other species display seasonal distribution patterns that can be tracked across years. Therefore, I hypothesize that the timing of the appearance of toxic species (e.g., *P. australis*) will be associated with the related environmental parameters (upwelling intensity and temperature) that vary at seasonal time scales.

Hypothesis III

Lastly, I hypothesize that changes in DA production (particulate DA and DA concentrations in shellfish tissue) will be correlated with changes in species assemblages, and in particular, with toxic species (such as *P. plurisecta* and *P. australis*), as well as with shifts in nutrient concentrations. In cultures and blooms, DA production has been shown to vary relative to the form and concentration of nutrients, and thus, I expect to see shifts in the concentration and ratios of dissolved nutrients in association with the onset and peak of DA toxicity.

Further, since *P. australis* appears to have a more northern origin (Scotian Shelf), I expect that *P. australis* will be observed first at the more coastal station (Bar Harbor) and then

inshore (MDIBL). To address the question of whether *P. australis* blooms are introduced via coastal rather than local assemblages, I hypothesize that if *P. australis* is observed first at the more coastal station (Bar Harbor) consistent with modeling by Clark et al, then that indicates a more northern origin (Scotian Shelf) of *P. australis* in the GOM.

To address these hypotheses, trends in species composition, cellular abundance, environmental conditions (temperature and salinity), hydrodynamic conditions (cumulative upwelling indices), nutrients (nitrate + nitrite, phosphate, and silicic acid) and toxin levels (DA in shellfish tissue and particulate DA) at two sites in the GOM during 2013-2020 were examined to inform ongoing observation and forecasting efforts and to further dissect *Pseudo-nitzschia* and DA dynamics in this region. This research will enhance early detection capabilities of toxic *Pseudo-nitzschia* species by outlining trends in species, nutrients, and environmental shifts, which will improve monitoring and potential mitigation strategies for this HAB-forming genus.

CHAPTER TWO:

LINKAGES BETWEEN *PSEUDO-NITZSCHIA* SPECIES DYNAMICS, DOMOIC ACID CONCENTRATIONS, AND ENVIRONMENTAL CONDITIONS IN THE GULF OF MAINE IN 2013-2020

Abstract

To better understand toxic *Pseudo-nitzschia* bloom dynamics across years with and without shellfish growing area closures, approximately weekly time series samples were collected in Bar Harbor and Mount Desert Island, Maine from 2013-2020. Samples were collected for analysis of *Pseudo-nitzschia* species composition and cell abundance, particulate domoic acid (DA), and dissolved inorganic nutrients. *Pseudo-nitzschia* species diversity was analyzed using Automated Ribosomal Intergenic Spacer Analysis (ARISA), a DNA fingerprinting method that showed dynamic interannual, seasonal and event-scale transitions in *Pseudo-nitzschia* species assemblages. For example, *P. australis* was only observed from 2016-2020, typically initiated during September of those years, and was associated with Maine shellfish growing area closures each year except 2020. Another species, *P. plurisecta*, typically dominated in late July and August, produced total particulate DA levels similar to that of *P. australis*, but has not caused any harvest closures to date in the United States. In contrast, *P. delicatissima* occasionally formed abundant blooms, most often in spring, that were not associated with DA. This ongoing research is critical for developing qualitative and quantitative

prediction capabilities for toxic blooms that account for changes in species diversity, leading to early warning systems and improved understanding of the potential drivers of toxin production.

Introduction

Harmful algal blooms (HABs) of the diatom genus *Pseudo-nitzschia* occur globally in estuarine, coastal, and offshore waters. There are over 59 species within the genus (Lelong et al., 2012; 52 described in Bates et al., 2018; 7 new species described in: Ajani et al., 2018; Huang et al., 2019; Dong et al., 2020; Chen et al., 2021; Percopo et al., 2022) and approximately half of these species can produce the neurotoxin, Domoic Acid (DA) (Bates et al., 2018) which is responsible for causing Amnesic Shellfish Poisoning (ASP) in humans and DA Poisoning (DAP) in wildlife. Upon consumption of DA-contaminated shellfish, humans may experience abdominal cramps, nausea, diarrhea, vomiting (Wright et al., 1989) and severe neurological issues such as disorientation, difficulty breathing, and permanent memory loss (Wright et al., 1989, Teitelbaum et al., 1990, Lelong et al., 2012), which can lead to death (Perl et al., 1990). DAP in wildlife such as fish, birds, and mammals can cause severe neurological dysfunction and mortality (Fritz et al., 1992; Work et al., 1993; Lefebvre et al., 1999; Scholin et al., 2000; Lefebvre et al., 2002) and DA toxicity can transfer through marine food webs by accumulation in wildlife (Bargu et al., 2002; Trainer et al, 2012). DA toxicity also has detrimental economic impacts due to shellfishery and fishery closures. For example, the first closure of the Dungeness crab fishery in Oregon as a result of high DA levels produced by a *P. australis* bloom resulted in a $97.5 million loss in revenue (Du et al., 2016; Moore et al., 2019).

The devastating human, wildlife, and economic impacts of toxic *Pseudo-nitzschia* blooms urges enhanced monitoring and identification of toxic *Pseudo-nitzschia* species in areas with emerging DA issues, such as the Gulf of Maine (GOM) where at least 14 *Pseudo-nitzschia* species have been confirmed (Fernandes et al., 2014). It is expected that there are more *Pseudo-nitzschia* species present in this region that have not yet been classified taxonomically. *Pseudo-nitzschia* was first observed in the 1920s and 1930s in the Georges Bank region of the GOM (Gran, 1993; Bigelow et al., 1940) and later reported throughout the GOM (Marshall and Cohn, 1981). Historically, this region experienced some low-level DA production events where shellfish tissue tested positive for DA but remained below the action limit of 20 µg DA g^{-1} tissue, which resulted in precautionary closures of shellfish growing areas (Bates et al., 2018). In 2016, the GOM experienced its first shellfish growing area closure due to shellfish tissue samples exceeding 100 µg DA g^{-1} tissue (Lewis et al., 2017). This widespread toxic event closed shellfish growing areas in the Bay of Fundy, Canada and led to precautionary closures in Massachusetts and Rhode Island (Bates et al., 2018). Prior research has shown that the novel presence of *P. australis* in this region was the primary culprit for the exceptionally high DA concentrations recorded in 2016 (Bates et al., 2018; Clark et al., 2019). In March 2017, Rhode Island experienced the second toxic *Pseudo-nitzschia* bloom and the confirmed presence of *P. australis* (Hubbard et al., 2017), leading to shellfish closures in this area. Since this event, *P. australis* and high DA levels have caused shellfish growing areas to close in Rhode Island and Maine in 2017 (Hubbard et al., 2017), and again in Maine in 2018 and 2019 (Clark et al., 2021).

Water mass anomalies are important drivers of *Pseudo-nitzschia* blooms (McCabe et al., 2016) and anomalously saline conditions in 2016 may be linked to the introduction of *P. australis* to the GOM region (Clark et al., 2019, 2021). Particle tracking models have shown that

inflows from the Nova Scotia Current likely introduced *P. australis* to the GOM system (Clark et al., 2021). This 2016 bloom was accompanied by increased salinity, greater ammonium concentrations, and lower residual silicic acid all of which were significantly different to prior years (Clark et al., 2019). During this 2016 bloom, upwelling-favorable winds may have reduced cell transport along the shore, resulting in *Pseudo-nitzschia* retention in the Bay of Fundy (Clark et al., 2019) which may have played a role in the major toxicity observed. The GOM system also experienced a "marine heat wave" in 2016 (Pershing et al., 2018; Clark et al., 2021) where sea surface temperatures in early October were greater than the 2001-2016 October mean (data from NERACOOS Buoy I; Clark et al., 2021). A similar phenomenon was observed in the vastly toxic 2015 U.S. West Coast *P. australis* bloom where surface water temperatures were 2.5 °C warmer than the long-term mean temperature in this region (McCabe et al., 2016). During this event, upwelled waters also had anomalously low silicate:nitrate which supported populations with high cellular DA (McCabe et al., 2016; Ryan et al., 2017).

For this study, field samples were collected approximately weekly at two sites on Mount Desert Island, Maine from 2013-2020 to identify temporal patterns among *Pseudo-nitzschia* species assemblages and environmental changes. *Pseudo-nitzschia* species composition, environmental conditions (temperature and salinity), nutrients (nitrate+nitrite, phosphate, ammonium, silicic acid), toxin levels (shellfish tissue DA and particulate DA) and cumulative upwelling indices were examined. Insight into the trends in species composition and how they relate to environmental shifts will enhance our ongoing monitoring efforts and improve our understanding of the underlying dynamics influencing this toxic HAB-forming genus.

Methods

Study sites

Whole seawater samples (n= 472) were collected weekly (Table 1) from Bar Harbor (44.43°N, -68.29°W) and Mount Desert Island Biological Laboratory (MDIBL) (44.39°N, -68.2°W), on Mount Desert Island, Maine from 2013-2020 (Figure 1). This region is well known for its hydrodynamic variability due to tides, wind, heat flux, and riverine discharge (Li et al., 2014). The study site map (Figure 1) was created using ArcGIS using a base map of the state of Maine obtained from Woods Hole Oceanographic Institute and importing latitude and longitudes for the study sites and shellfish harvest areas obtained from Maine Department of Marine Resources.

Table 1. Total number of samples (n=472) collected at the Bar Harbor and MDIBL sites across years.

	Bar Harbor	Sampling months	MDIBL	Sampling months
2013	19	June-October	20	June-October
2014	29	April-October	31	May-October, December
2015	26	February-September	17	June-September
2016	25	June-November	27	June-October
2017	37	May-December	41	February-December
2018	27	May-November	40	January-October
2019	36	March-November	34	March-November
2020	37	February-November	26	May-November

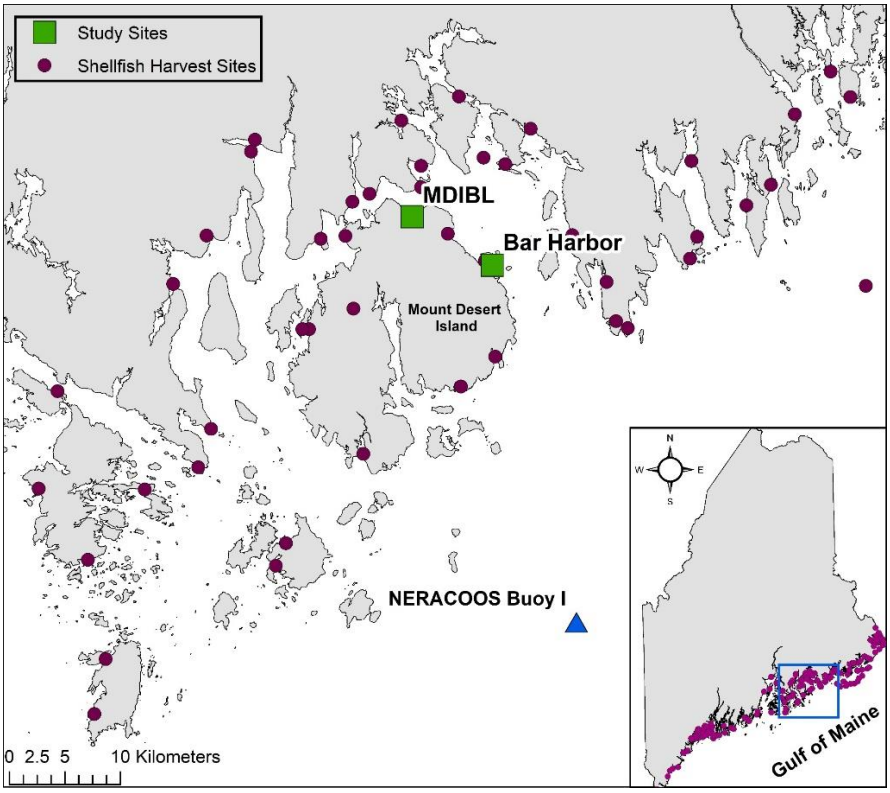

Figure 1. Study sites in Mount Desert Island, Maine shown in green boxes. Shellfish growing area sites collected by Maine Department of Marine Resources (DMR) shown in purple circles. NERACOOS Buoy I is indicated by blue triangle.

These two sampling sites in this study are located on an inshore area that is influenced by the Gulf of Maine Coastal Current, which is divided into the Eastern Maine Coastal Current (EMCC) (east of the Penobscot River) and Western Maine Coastal Current (WMCC) (west of the Penobscot River) and flows east to west (Pettigrew et al., 2005; Townsend et al., 2015). Bar Harbor and MDIBL sites reside just east of this dividing line where they receive cold and nutrient-rich waters from the EMCC (Brooks and Townsend, 1989). The EMCC has been shown to branch off into two parts; one portion turns offshore near Penobscot Bay and contributes to the cyclonic circulation around the Jordan Basin while the other portion continues southwestward along the coast and contributes to the WMCC (Brooks and Townsend, 1989; Bisagni et al. 1996;

Pettigrew et al., 1998, 2005). Two major cyclonic gyres in the Jordan and Georges Basins exist further offshore and may increase residence times in the eastern portion of the GOM (Pettigrew et al., 2005). The study sites are also influenced by different water masses flowing in from the northeast, such as cold and relatively fresh Scotian Shelf waters (Townsend et al., 2015) and riverine input from the Penobscot River, Kennebec River, Androscoggin River, St. John River, and Merrimack River (Li et al., 2014).

Hydrodynamic measurements

Hourly buoy data was obtained from the Northeastern Regional Association of Coastal Ocean Observing Systems (NERACOOS). Temperature and salinity were obtained from NERACOOS Buoy I (44.10°N, - 68.11°W) (Figure 1) at 1 m below the sea surface and are referred to "offshore" temperature and salinity in the text. Cumulative upwelling indices (CUI) were calculated by integrating upwelling indices over time from June through October in each year from 2013-2018 using methods described in Li et al. (2014). Buoy I data for 2019-2020 was not available.

Sample collection

Cell abundance, temperature, and salinity were measured as part of the Maine Department of Marine Resources' monitoring program. Temperature and salinity were measured upon sample collection using YSI probes and are referred to as "inshore" temperature and salinity in the text. *Pseudo-nitzschia* species, as well as other phytoplankton genera such as *Alexandrium*, *Dinophysis* and other notable species, were enumerated using an inverted light microscope. Upon collection, 10 L of seawater was filtered through a 20 μm sieve which was then inverted and held over a funnel attached to a 50 mL Falcon tube and gently rinsed with

seawater from the site to obtain 15 mL of concentrated seawater. The sample was then preserved with unacidified Lugol's solution before enumeration.

ARISA DNA fragment analysis

For DNA samples, 125 mL aliquots of each whole seawater sample were filtered onto 0.45 µm pore size nitrocellulose filters (Millipore) and the filters were stored in cryogenic vials at -80 °C until processed. Genomic DNA was extracted from the filters using a DNeasy Plant Mini Kit (Qiagen Inc.) using the provided instructions. Genomic DNA was quantified following extraction by adding 1 µL of genomic DNA to 49 µL of TE Buffer (10 mM Tris-HCl and 0.5 mM EDTA added to sterile nanopure water and autoclaved) then adding the DNA in TE to 50 µL of a 1:200 mixture of fluorescent PicoGreen (Invitrogen) reagent in TE Buffer. Fluorescence of each sample was then measured using a Synergy H1 plate reader (BioTek Instruments, Inc.) and DNA concentrations were calculated using Gen5 software (BioTek Instruments, Inc.). Samples were standardized to 1 ng μL^{-1} and 10 ng of the standardized genomic DNA was added to 20 µL triplicate PCR reactions using genus-specific primers Pnall F (5′-TCTTCATTGTGAATCTGA-3′) and FAM-labeled Pnall R (5′-CTTTAGGTCATTTGGTT-3′; Eurofins Genomics) (Hubbard et al., 2008). PCR reactions followed the method described in Hubbard et al. (2014) which consisted of 2.5 mM deoxynucleoside triphosphates, 0.4 mM of each primer, 0.75 U of Apex Taq polymerase, 2 mM of $MgCl_2$, and 1 X standard reaction buffer (Apex Bioresearch Products). PCR amplifications consisted of a 2-minute denaturation step at 94 °C, followed by 32 cycles of 30 seconds at 95 °C, 30 seconds at 50.6 °C for annealing, and 60 seconds at 72 °C, followed by a 10 minute extension at 72 °C. PCR products were purified by adding 80 µL of TE buffer to each 20 µL PCR product and loading it onto MultiScreen PCR 96

filter plates (Millipore) with a vacuum pump attached. Purified PCR products from each triplicate reaction of the same target DNA were eluted using molecular biology grade nuclease-free water (Fisher Scientific) and pooled together. Following purification, samples were quantified using PicoGreen and the Synergy H1 plate reader as described above. PCR products were standardized to 1 ng μL^{-1} and analyzed on an Applied Biosystems 3730 XL DNA Analyzer (University of Illinois DNA Core Sequencing Facility) using a LIZ600 size standard for DNA fragment analysis. DAx software (Van Mierlo Software Consultancy) was used to analyze electropherograms to distinguish amplicon sizes. Due to cell size differences, this method approximates the relative amount of DNA contributed from each species rather than cellular abundance. Relative abundance of each amplicon size was calculated based on ARISA profiles and ARISA fragments were assigned to species based on known GOM *Pseudo-nitzschia* sequences (as in Hubbard et al. 2008, 2014). Novel ARISA fragments that do not have putative taxonomic identifications associated with them are referred to in the text as "Unknown" followed by the number of base pairs in the species' internal transcribed spacer 1 (ITS1) region detected by ARISA (for example, Unknown 148).

Particulate domoic acid (pDA)

For pDA samples, 250 mL aliquots of each whole seawater sample were filtered onto 47 mm GF/F filters (Whatman), which were stored in 2 mL cryogenic vials at -80 °C until analysis. Prior to extraction, filters were transferred to 15 mL polypropylene centrifuge tubes using sterile forceps. Particulate domoic acid was extracted by adding 5 mL of 20% aqueous MeOH to each tube, vortexing for 2 minutes, and centrifuging at 3500 x g at 4 °C for 10 minutes. The supernatant was then transferred to a glass vial and stored in the dark at -20 °C until analyzed.

Extracts were analyzed following the protocol described in Lopez et al. (2021). Briefly, pDA extracts were filtered through 0.22 µm PVDF syringe filters and analyzed using an Acquity ultra-high performance liquid chromatographic (UPLC) system coupled to a Quattro Micro™ API triple quadrupole mass spectrometer (MS) (Waters, Milford, MA, USA). An Acquity UPLC BEH C18 1.7 µm column (2.1 x 100 mm) was used to perform separations with an injection volume of 10 µL, a flow rate of 0.4 mL/min, and a column oven temperature of 40 °C. Mobile phase A consisted of a 0.1% formic acid solution in water, and mobile phase B was acetonitrile with 0.1% formic acid. Gradient conditions included 5% mobile phase B for 0.3 minutes, followed by a linear gradient to 40% B at 2.5 minutes before returning to initial conditions at 3 minutes and reconditioning the column for 1 minute. The following parameters were used to operate the MS in positive ionization mode (ESI+) capillary voltage 3.5 kV, cone voltage 28 V, desolvation temperature 500 °C, and desolvation gas flow 850 L/h. From the protonated DA ion, multiple reaction monitoring transitions were monitored for the transitions: *m/z* 312 > 193, *m/z* 312 > 248, and *m/z* 312 > 266; and the collision energies were optimized for each precursor/product pair. To generate the 8-point standard curve for quantitation of DA, a certified reference standard solution of DA was used (National Research Council, Halifax, Canada).

Shellfish tissue domoic acid

Domoic acid data from mussel (*Mytilus* genus) tissue were provided by the Maine Department of Marine Resources and contain data from shellfish growing areas along the Maine coast, including ones from east and west of the Bar Harbor and MDIBL study sites (Figure 1).

Nutrients

Nutrient samples were collected from 2013-2016 and January-July 2017 by filtering whole seawater samples through a 0.22 µm PVDF luer-lock syringe filter and stored in vials at -20 °C until analysis. Nutrient samples in August 2017-2020 were collected using 0.45 HA nitrocellulose filters inside a Swinnex filter holder and luer-lock syringe and stored at -20 °C until analysis. Samples were then sent to nutrient facilities at the University of Maine (2013-2017) and Woods Hole Oceanographic Institute (2018-2020) and were analyzed for nitrate + nitrite (NO_x^-), ammonium (NH_4^+), silicic acid ($Si(OH)_4$), and phosphate (PO_4^{3-}) concentrations. Due to the nature of nitrocellulose filters, it is possible to have nitrate leaching from the filters which would interfere with nitrogen measurements. Another variable is that these two filter types had different pore sizes. In the text, nutrients are referred to as NO_x (nitrate+nitrite), ammonium (ammonium), Si (silicic acid), and P (phosphate).

Descriptive analyses

To identify seasonal changes in *Pseudo-nitzschia* species assemblages, months were categorized into seasons as follows: winter = December, January, February; spring = March, April, May; summer = June, July, August; fall = September, October, November.

Statistical analyses

Spearman's Rank Correlation Coefficient (Rho) was calculated using IBM SPSS Statistics for Windows (IBM Version 26.0, IBM Corp., Armonk, NY, USA) to evaluate relationships between environmental parameters (temperature, salinity, DA, NO_x, ammonium, Si, P, dissolved inorganic nitrogen (DIN), residual nitrate and ammonium, and nutrient ratios)

and *Pseudo-nitzschia* species identified by ARISA. Spearman's Rho was calculated for each study site individually and for both sites combined.

PRIMER 7 software (v. 7.0.17, PRIMER-E, Auckland, New Zealand) was used for the following statistical analyses: non-metric dimensional scaling (nMDS), Analysis of Similarity (ANOSIM), Principle Component Analysis (PCA), and BVSTEP (step-wise BIOENV). Prior to analyses, samples from Bar Harbor and MDIBL sites were pooled together since ANOSIM results showed that the assemblages at the two sites did not differ significantly. Only samples that contained ARISA data were selected (n=393) and rare taxa, defined as taxa in <5% of samples, were removed to reduce noise and highlight patterns in species assemblages. Bray-Curtis similarity index was calculated for *Pseudo-nitzschia* species abundances to quantify compositional similarities across samples. Prior to analysis, environmental variables (NO_x, Si, P, ammonium, nutrient ratios, and domoic acid) were fourth root transformed to approach normal distributions. Temperature and salinity data were not transformed as these variables exhibited close to normal distributions. Once the nutrient variables and DA were transformed, all environmental variables, including temperature and salinity, were normalized relative to each other to approach normal distributions.

Non-metric multidimensional scaling (nMDS) was used to investigate potential biological and environmental indicators of *Pseudo-nitzschia* species assemblage patterns. This approach was chosen because it is well suited for non-normally distributed data which is common for species abundance data. The distance between sample points on the plots indicates the similarity (or dissimilarity) in species composition. For example, samples that ordinate closer together indicate higher similarity. Vectors representing environmental variables or species were

superimposed on the nMDS plots to indicate the direction in which the variable is increasing. The length of the vector represents the magnitude of the correlation between the variable and species composition (Rothenberger et al., 2009). There was lower sampling resolution in winter and some spring months (December-April). To ensure that the data were not being skewed by reduced sampling during this timeframe, nMDS ordination was conducted only for higher resolution sampling months (July-October) and the same patterns were observed. Thus, nMDS results for the full data set are presented in results section.

Analysis of Similarity (ANOSIM) was used to compare and quantify differences in species and environmental data across years (2013-2020) and seasons (spring, summer, winter, and fall). Due to the use of the nitrocellulose filters for nutrient sample collection in 2017-2020 (discussed in the nutrient methods section) the environmental data were handled in 2 ways: full environmental dataset (includes all nutrient data) and partial environmental dataset (only includes data from 2013-2016 and January-July 2017, which encompasses nutrient samples collected with established methods). In the results and discussion sections, these 2 sets are referred to as “full environmental data” and “partial environmental data”.

To visualize the patterns of environmental data, Principle Components Analysis (PCA) was conducted and relationships were further analyzed with PERMANOVA to investigate statistical significance of the following groupings: seasons, years, and seasons within years. PERMANOVA results matched ANOSIM results and did not reveal anything different, therefore only the results from ANOSIM and PCA are presented in the results section.

The most highly correlated species to each season (spring: n=69; summer: n=185; fall: n=128; winter: n=12) were identified using the BVSTEP (step-wise BIOENV) procedure in

PRIMER 7. This method used the Spearman rank correlation to correlate patterns in the species data using the Bray-Curtis distance matrices.

Results

Cellular abundance

Pseudo-nitzschia cellular abundance varied across years at both sites. The highest cell concentrations were observed in 2017 and the 2018 bloom had the lowest peak concentration observed (Figure 2, Table 2). In Bar Harbor, peak concentrations were observed in summer-fall months of June (2014, 2016, 2017, 2019), August (2015), September (2013, 2018), and October (2020) (Table 2). In MDIBL, peak concentrations occurred in June (2017, 2019), July (2018), August (2013, 2015), and October (2014, 2016, 2020). High cell concentrations (>100,000 cells L^{-1}) of *Pseudo-nitzschia* typically lasted 1-7 weeks (Table 2).

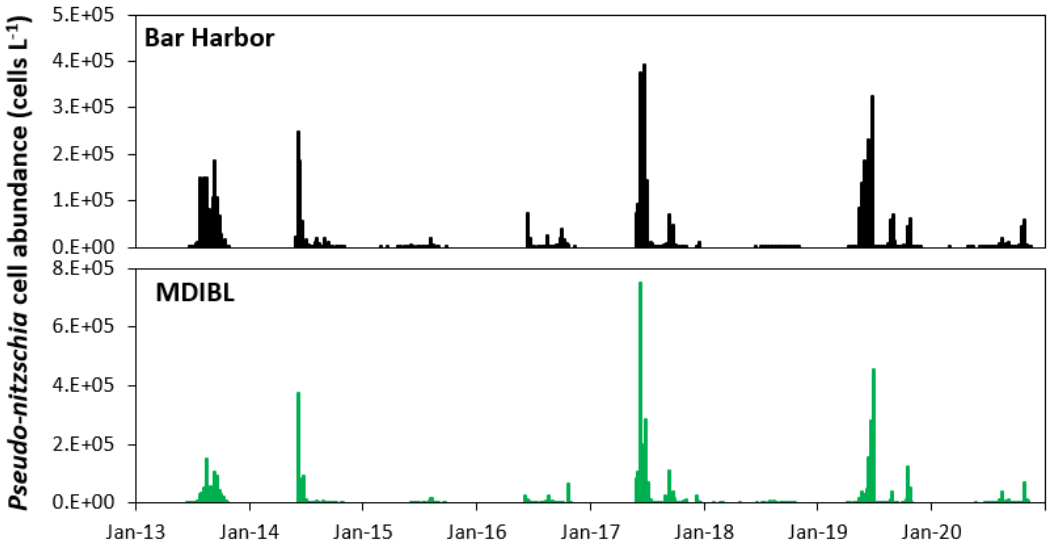

Figure 2. *Pseudo-nitzschia* cellular abundance in Bar Harbor and MDIBL from 2013-2020.

Table 2. Peak *Pseudo-nitzschia* cellular abundance (cells L^{-1}) and number of weeks with high concentrations (>100,000 cells L^{-1}).

	Bar Harbor		MDIBL	
	Maximum cell concentrations (cells L^{-1})	**Weeks with cells >100,000 cells L^{-1}**	**Maximum cell concentrations (cells L^{-1})**	**Weeks with cells >100,000 cells L^{-1}**
2013	187,500	7	150,000	2
2014	250,000	2	375,000	1
2015	21,429	0	17,442	0
2016	75,000	0	68,182	0
2017	392,250	3	750,000	6
2018	4,950	0	8,350	0
2019	326,400	6	456,750	4
2020	59,654	0	70,125	0

Species assemblages and succession

At the Bar Harbor site, ARISA detected 18 different fragments or taxa, 11 that were attributed to known GOM *Pseudo-nitzschia* species and 7 that were not identified based on known GOM diversity (Figure 3) and are described as "Unknown" followed by the fragment size detected by ARISA (base pairs). In each year, 8-12 taxa were observed. In Bar Harbor, *P. pungens* and *P. plurisecta* were observed each year and *P. seriata* and *P. delicatissima* were observed each year except for 2018. *P. cuspidata* often was observed in each year, with the exception of 2014 and 2019. At the MDIBL site, ARISA detected 20 fragments, 12 of which were known GOM *Pseudo-nitzschia* species, 8 of which were not identified using GOM sequences and are described as "Unknown" as mentioned previously (Figure 3).

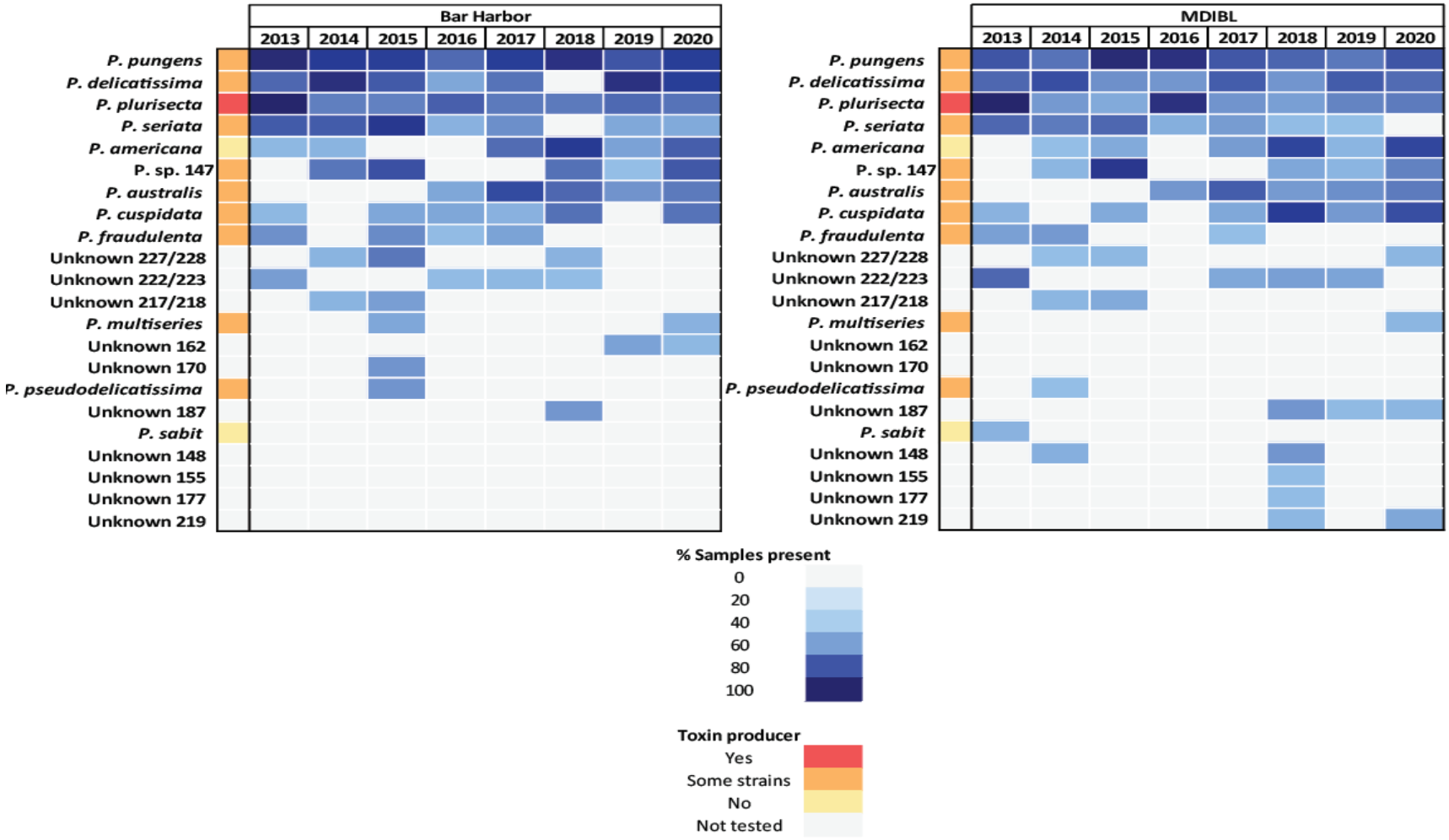

Figure 3. *Pseudo-nitzschia* species present at both sites from 2013-2020. Each bar represents species presence and the shade of blue of the bar shows the percentage of samples that the species is present in. Whether or not the species has been shown to produce toxin is represented by a yellow-red color in the column directly next to the species name and corresponds to the toxin producer legend at the bottom of the figure.

The minimally toxic species, *P. pungens* and *P. delicatissima*, were observed each year. The toxic species *P. plurisecta* was observed in all years, *P. seriata* was observed each year except for 2020, and *P. australis* was observed each year since 2016. *P. americana* was observed each year except for 2013 and 2016 and *P. cuspidata* was observed each year except for 2014 and 2016. Species richness peaked in 2015 in Bar Harbor where ARISA detected 12 taxa including one taxon that was found only in that year (unknown 170 bp). At the MDIBL site, 2018 had the highest species richness with 14 taxa observed, including 2 taxa that have only been observed in that year (unknowns 155 bp and 177 bp).

Seasonal and episodic species succession patterns were observed, and notable trends are described here. Seasonal species succession was observed in all years at both sites. *P. delicatissima* and/or P. sp. 147 were associated with cooler waters in the spring with mean inshore seawater temperatures across years ranging from 5.1-8.3 °C and mean inshore salinities ranging from 30.3-33.3 during this season at both sites (Table 3). *P. delicatissima* occasionally formed abundant blooms, most often in spring, that were not associated with DA. In summer and into early fall months, the species assemblage shifted to include *P. pungens, P. plurisecta,* and in most years, *P. seriata* (Figures 4 and 5) where mean inshore temperatures typically ranged from 13.5-15.5 °C in summer and 12.2-15.1 °C in fall and mean inshore salinities ranged from 30.5-32.7 in summer and 31.3-34.1 in fall (Table 3). There were two exceptions to this "typical" summer/fall assemblage – one of which was observed in both sites in 2018 where the late summer/early fall assemblage consisted of *P. pungens, P. plurisecta,* and *P. americana.* The second exception was observed at the MDIBL site in 2020 where *P. seriata* was not observed and the late summer/early fall assemblage consisted of *P. pungens, P. plurisecta,* and *P. delicatissima*; this fall season in 2020 was accompanied by lower mean temperatures compared

to 2013-2018. Besides these exceptions, the typical summer/fall assemblage of *P. pungens, P. plurisecta,* and *P. seriata* continued through late fall/early winter in 2013-2015.

Table 3. Seasonal inshore mean temperature and salinity for Bar Harbor and MDIBL sites combined. Areas with dashes indicate that there were no data available to calculate means.

	Winter	Spring	Summer	Fall
Temperature (°C)				
2013	-	-	14.5	13.2
2014	-	7.9	14.7	13.3
2015	-	5.1	13.5	15.1
2016	-	-	14.3	14.1
2017	5.6	8.3	13.7	13.3
2018	2.3	8.0	15.1	12.8
2019	-	6.1	14.3	11.8
2020	2.0	7.1	15.5	12.4
Salinity				
2013	-	-	32.1	34.1
2014	-	31.5	31.2	32.4
2015	-	32.7	31.5	31.3
2016	-	-	32.1	32.1
2017	32.1	30.3	31.0	32.2
2018	33.0	31.1	31.0	31.4
2019	-	30.5	30.5	32.3
2020	34.0	33.3	32.8	34.2

Sharp transitions in species assemblages were observed on a weekly scale. For example, at the Bar Harbor site in July 2013, *P. pungens* was the only species detected until two weeks later when the assemblage expanded to include *P. seriata, P. plurisecta,* and *P. delicatissima.* In the same year, another shift was observed in September, where *P. pungens, P. seriata,* and *P. plurisecta* made up the species assemblage and then 1.5 weeks later the assemblage expanded to include *P. fraudulenta* and unknown 222/223 with the disappearance of *P. seriata.* Another rapid transition that was observed was in the fall assemblage of 2014 at the MDIBL site where the species assemblage shifted to include *P. fraudulenta* along with the continued observance of *P. seriata* and *P. pungens.* During this time frame at the Bar Harbor site, the usual fall assemblage

of *P. pungens, P. plurisecta,* and *P. seriata* was observed and *P. fraudulent* was not observed. Then, in the following year's winter/spring months, the species assemblage in Bar Harbor shifted to *P. fraudulenta* with the continued observance of *P. pungens, P. plurisecta,* and *P. seriata.* Therefore, we saw a species assemblage shift first at the MDIBL site and subsequently observed the same shift at the Bar Harbor site. Another shift that was observed first at the MDIBL site was in 2020 where the species assemblage on October 1st was comprised of *P. australis, P. americana,* and *P. pungens* but then shifted to include *P. multiseries* and *P. cuspidata* as part of the species assemblage the following week on October 7th. This shift was observed in Bar Harbor a week later on October 15th.

Multiple toxic species such as *P. plurisecta, P. seriata, P. pungens,* and *P. australis* often co-occurred in the same sample. *P. plurisecta* typically dominated in late July and August and is known to produce total pDA levels similar to that of *P. australis* in this region but has not caused any shellfish growing area closures to date in the United States. *P. seriata* dominated the species assemblage in samples from Bar Harbor in late September-October in years prior to 2016. Besides 2017, where *P. seriata* was dominant in 2 weeks in August in Bar Harbor and 1 week in August in MDIBL, *P. seriata* was seen in relatively small proportions and did not dominate any samples at either site in years after 2016. *P. pungens* typically dominated in the late summer/fall months of July-September. In 2016 and all succeeding years, *P. australis* became the dominant species in the assemblage at both sites, typically beginning in September (Figures 4 and 5).

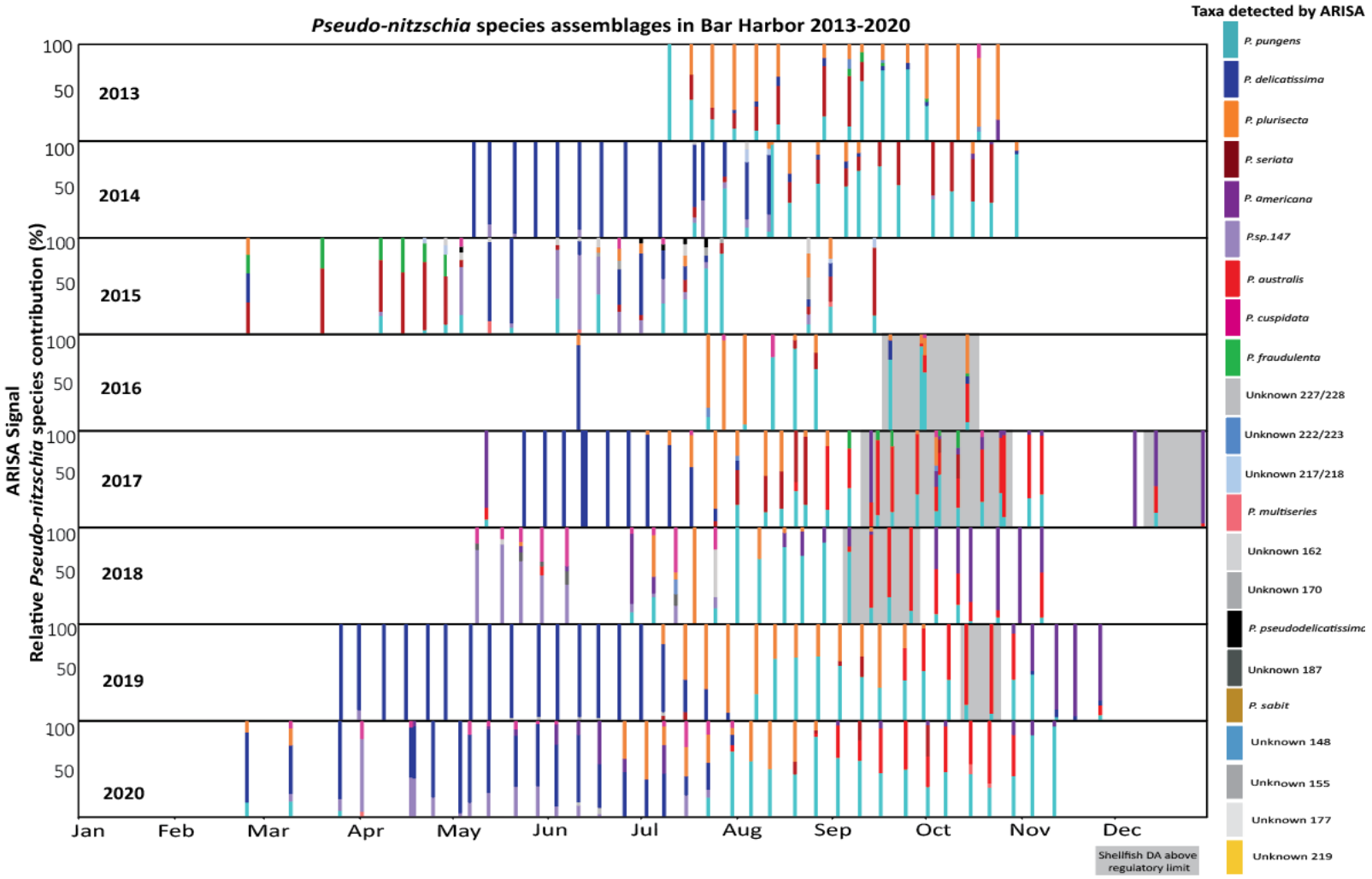

Figure 4. *Pseudo-nitzschia* species assemblages in Bar Harbor from 20130-2020. Each vertical line represents one sample and each color in the line represents the relative proportion of each species in the sample. Areas with no vertical lines means there were no samples collected.

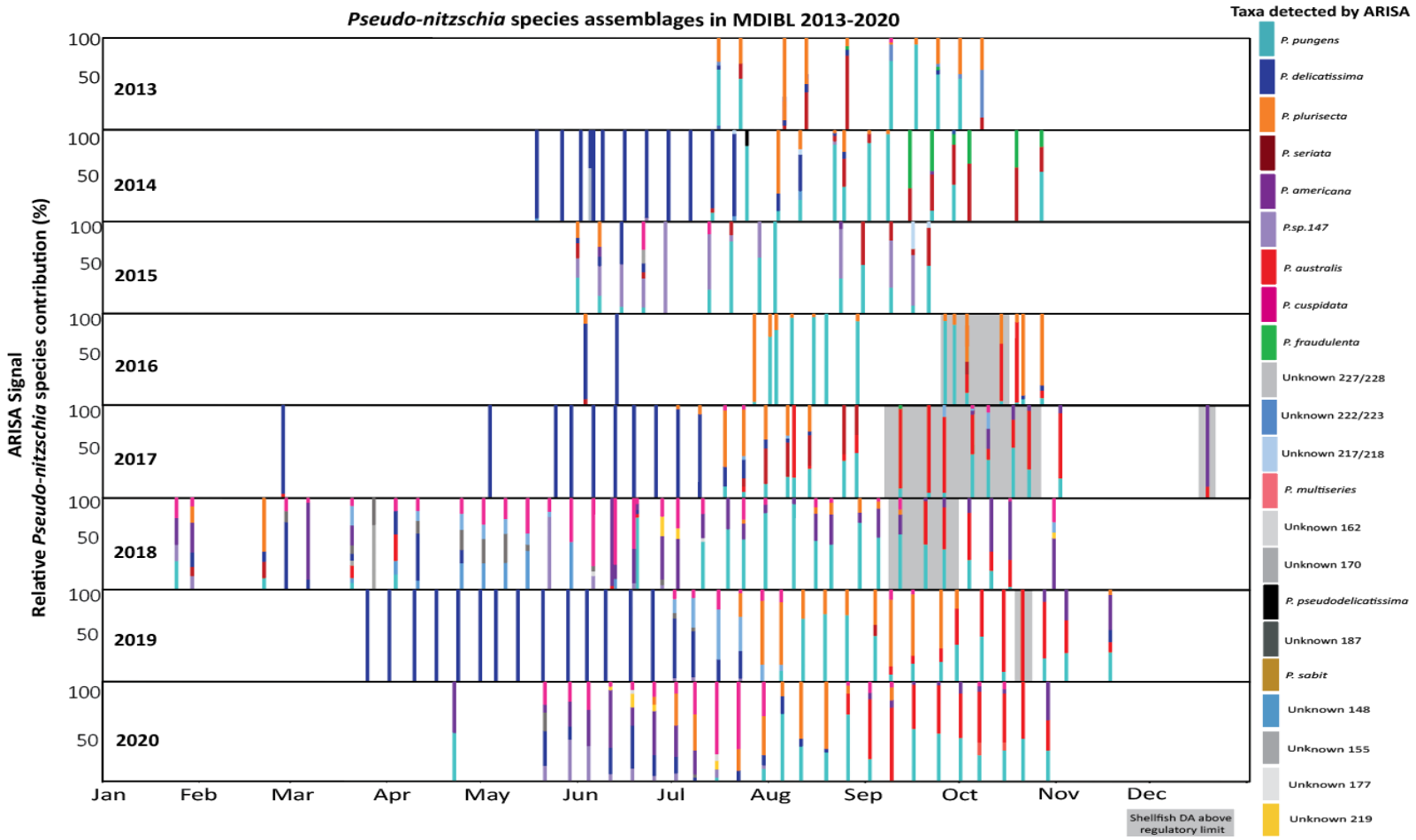

Figure 5. *Pseudo-nitzschia* species assemblages in MDIBL from 2013-2020. Each vertical line represents one sample and each color in the line represents the relative proportion of each species in the sample. Areas with no vertical lines means there were no samples collected.

Timing and niche of *P. australis*

The timing and duration of *P. australis* observance varied across years and across the two sites. *P. australis* was observed in some samples sporadically throughout the years but did not always became part of the assemblage for an extended period of time. For example, in 2018, *P. australis* was only observed in two samples in March, one sample in April, and two samples in June. Therefore, the dates that *P. australis* was observed and also persisted and became part of the assemblage for at least 2 consecutive weeks are highlighted here. Blooms of *P. australis* occurred earlier in the year in 2017-2020 than in 2016. The first observance of *P. australis* alternated between sites each year except for 2020 when *P. australis* was first observed simultaneously at both sites on August 26th (Figure 6). In 2016, *P. australis* was first observed in Bar Harbor on September 26th. In 2017, *P. australis* was first observed in MDIBL on August 9th. The first observance of *P. australis* in 2018 was in Bar Harbor on September 6th and the first observance of *P. australis* in 2019 was in MDIBL on September 9th. Besides *P. australis*, there were no other novel species observed at either site in 2016.

To determine which *Pseudo-nitzschia* species coexist with *P. australis*, species assemblages were observed during the periods described above (when *P. australis* was first observed and also persisted in the assemblage for at least two consecutive weeks). At both sites, *P. pungens* and *P. plurisecta* were observed with *P. australis* in 2016-2020 and *P. americana* was observed in four out of five years (2017, 2018, 2019, 2020). *P. cuspidata* was also observed in four out of five years at the MDIBL site (2017, 2018, 2019, 2020). *P. multiseries* was observed at both sites only in 2020 and *P. seriata* co-occurred with *P. australis* in 2017 and 2020 at Bar Harbor and in 2016 and 2017 at MDIBL.

Broad temperature and salinity ranges were observed during periods of *P. australis* presence and varied across years. To better examine the temperature and salinity niche of *P. australis*, the dataset was constrained to only include samples with inshore temperature and salinity data from the same months across all years, in an attempt to avoid bias in the data due to variability in sampling months across years. With the constrained dataset, *P. australis* was observed in 11-18.3 °C and 28-35 salinity across years (Table 4).

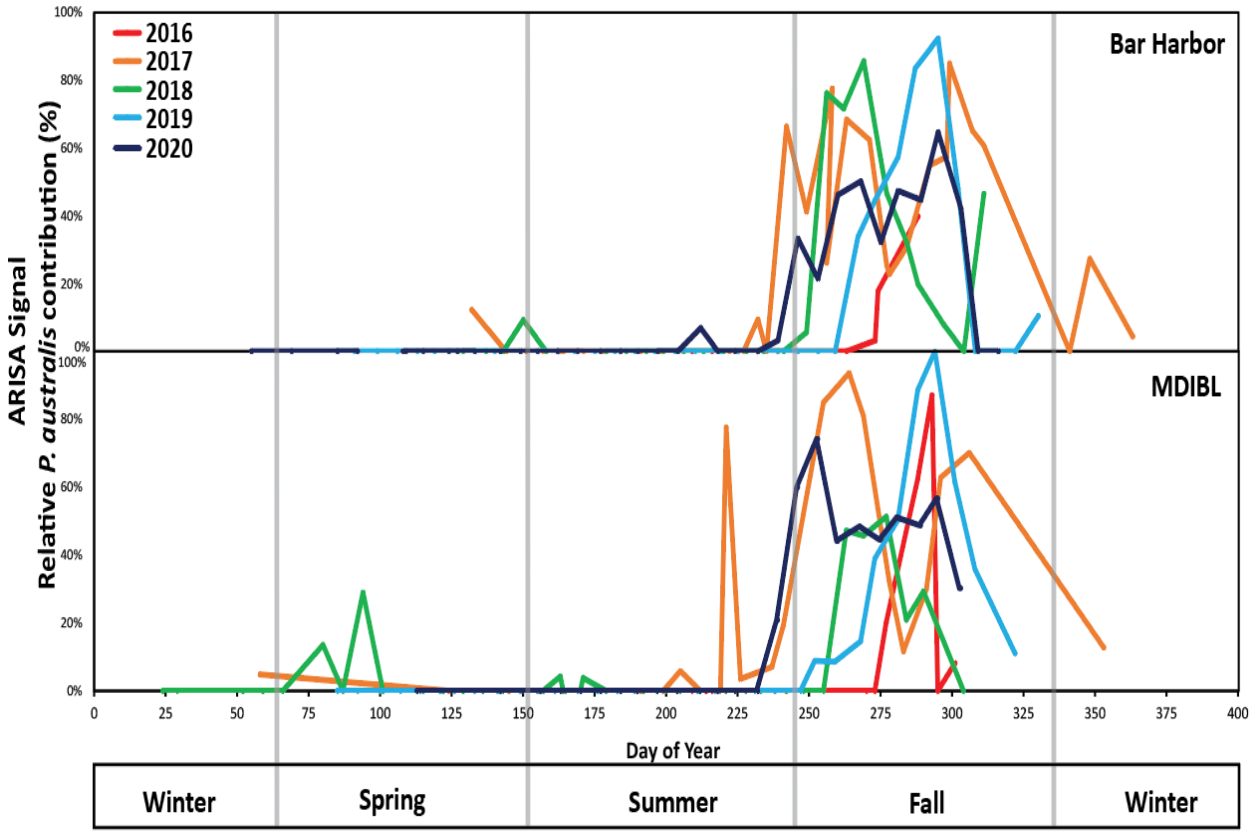

Figure 6. Timing of *P. australis* observance at Bar Harbor and MDIBL from 2016-2020.

Table 4. Temperature and salinity ranges during periods of *P. australis* presence at both sites during September-October.

	Bar Harbor		MDIBL	
	Temperature range (˚C)	**Salinity range**	**Temperature range (˚C)**	**Salinity range**
2016	11.9 – 13.3	32 – 33	11.4 – 14.1	32 – 33
2017	12 – 14.4	31 – 32	12.4 – 18.3	31 – 32
2018	11 – 15.9	28 – 33	12.4 – 15.4	30 – 33
2019	11.5 – 13.7	32 – 33	11.5 – 14.8	32 – 33
2020	11 - 15	33 – 35	11 – 16.4	33 – 35

Particulate domoic acid and shellfish tissue domoic acid

Particulate domoic acid varied considerably from year to year. Peak concentrations of DA in Bar Harbor reached 1.2 µg L^{-1} in 2013, 0.15 µg L^{-1} in 2014, 0.04 µg L^{-1} in 2015, 0.13 µg L^{-1} in 2016, 2.43 µg L^{-1} in 2017, 0.09 µg L^{-1} in 2018, 1.8 µg L^{-1} in 2019, and 0.79 µg L^{-1} in 2020 (Figure 7). In MDIBL, peak DA concentrations reached 0.76 µg L^{-1} in 2013, 0.03 µg L^{-1} in 2014, 0.02 µg L^{-1} in 2015, 1.51 µg L^{-1} in 2016, 2.87 µg L^{-1} in 2017, 0.05 µg L^{-1} in 2018, 3.22 µg L^{-1} in 2019, and 1.55 µg L^{-1} in 2020 (Figure 7). The highest pDA concentrations were observed mostly in the fall season across all years and both sites. One exception is in 2013 at the Bar Harbor site, where the maximum pDA concentration was in the summer (August) due to a *P. plurisecta* bloom in that year.

The maximum shellfish tissue toxin concentrations were 2.28 µg g^{-1} in 2014, 5.5 µg g^{-1} in 2015, 128.6 µg g^{-1} in 2016, 60.4 µg g^{-1} in 2017, 42 µg g^{-1} in 2018, 22.2 µg g^{-1} in 2019, and 8.5 µg g^{-1} in 2020 (Figure 7). Shellfish harvest closures due to DA levels over the regulatory limit (> 20 µg g^{-1} shellfish tissue) occurred in association with *P. australis* from 2016-2019 with interannual differences in the severity and duration of events. At both sites, *P. australis* persisted

for approximately 6 weeks in 2016, 15 weeks in 2017, and 6 weeks each in 2018 and 2019. Shellfish tissue toxin remained above the regulatory limit for 4 weeks in 2016, 15 weeks in 2017, 2 weeks in 2018, and 1 week in 2019. Although *P. australis* persisted for 9 weeks in 2020, there were no shellfish growing area closures in that year.

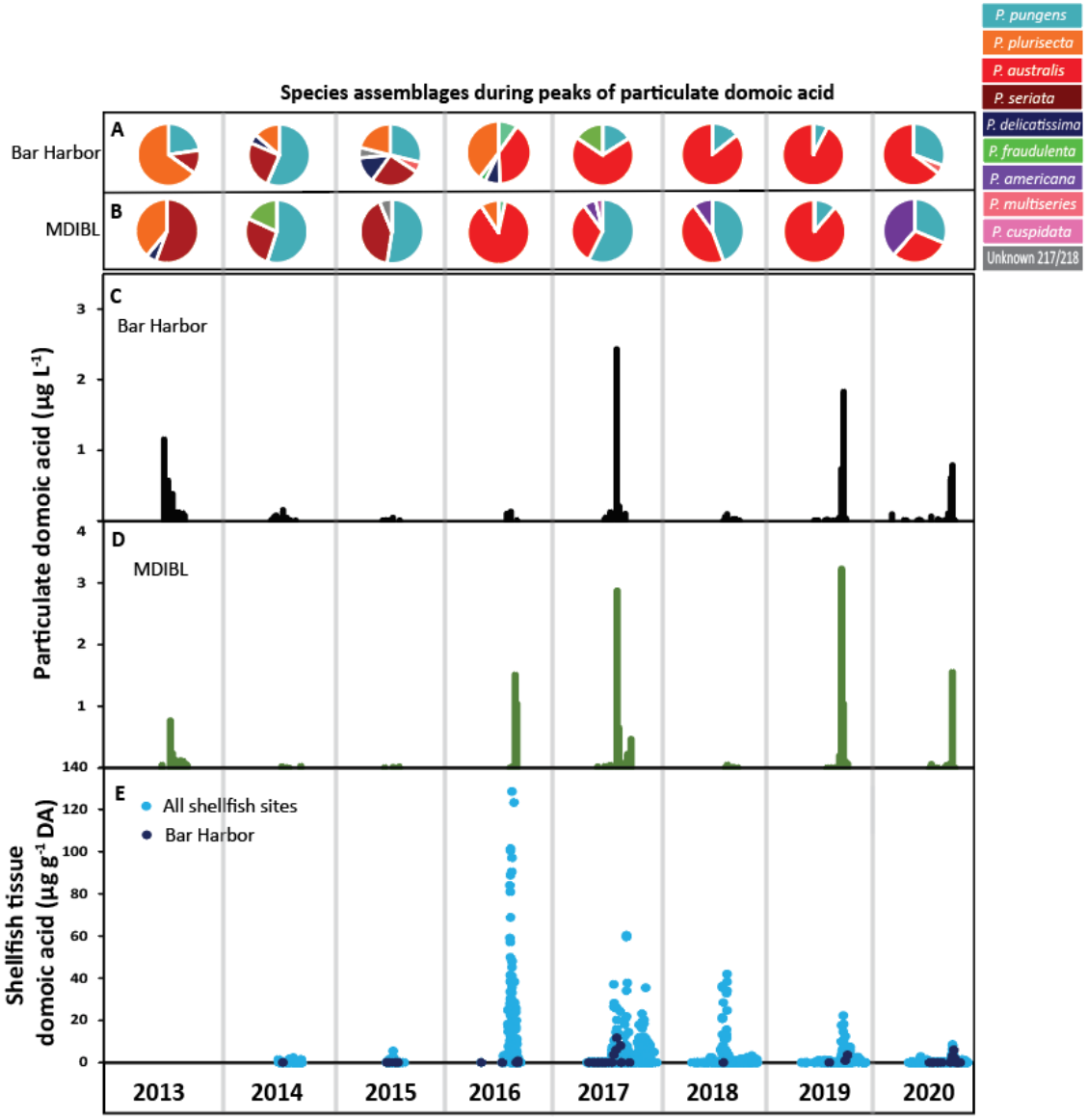

Figure 7. *Pseudo-nitzschia* species observed during peaks of particulate domoic acid at Bar Harbor (BH) (A) and MDIBL(B). Particulate domoic acid concentrations at Bar Harbor (C) and MDIBL (D) and domoic acid from shellfish tissue (E).

The highest levels of pDA were observed in 2017 at the Bar Harbor site and in 2019 at the MDIBL site, whereas the highest levels of shellfish tissue toxin were recorded in 2016. As previously mentioned, toxin levels in shellfish tissue never exceeded the regulatory threshold in 2020, despite considerable pDA levels detected in seawater which persisted for 14 weeks. Shellfish tissue toxin results indicated a gradual decrease in DA concentrations after the 2016 event in the GOM (Figure 7). However, pDA levels remained detectable after 2016 and a downward trend in pDA concentration was not observed at either site (Figure 7).

Species assemblages were examined during peak pDA concentrations at both sites (Figure 7). In 2013, peak pDA concentrations were associated with *P. plurisecta* and *P. seriata* at both sites, with the addition of *P. pungens* in Bar Harbor and *P. delicatissima* in MDIBL. The following year was dominated by *P. pungens* and *P. seriata* with the addition of *P. plurisecta* and *P. delicatissima* at Bar Harbor, and *P. fraudulenta* at MDIBL. In Bar Harbor in 2015, multiple toxic species were present during peak pDA concentrations including *P. plurisecta, P. pungens, P. seriata, P. multiseries.* Other species present at this site include *P. delicatissima* and Unknown 217/218 bp. At the MDIBL site, the assemblage consisted of *P. pungens, P. seriata,* and Unknown 217/218 bp. In 2016, peak pDA concentrations were associated with *P. pungens, P. plurisecta,* and *P. australis* at both sites. In years after 2016, *P. australis* and *P. pungens* were prevalent at both sites during maximum pDA concentrations. Other species that were present included *P. fraudulenta* (Bar Harbor) and *P. americana* and *P. cuspidata* (MDIBL) in 2017; *P. americana* (MDIBL) in 2018 and 2020; and *P. multiseries* (Bar Harbor) in 2020 (Figure 7). A clear shift was observed between years prior to 2016 where samples at peak pDA were dominated by *P. pungens*, *P. plurisecta*, or *P. seriata* and years after 2016 where samples were dominated by *P. pungens* and *P. australis* (Figure 7).

Statistical analysis – Spearman's rank

Spearman's analysis was conducted on each site individually as well as on both sites combined and revealed significant relationships between taxa and environmental factors. At the Bar Harbor site, 2 taxa (*P. pungens* and *P. seriata*) were positively correlated with both temperature and salinity and *P. plurisecta* was positively correlated with temperature only. Negative correlations between 4 taxa (*P.* sp. 147, *P. delicatissima, P. fraudulenta,* and Unknown 228) and temperature were observed. *P. delicatissima* was negatively correlated with salinity whereas *P. fraudulenta* was positively correlated with salinity (Table 5). At the MDIBL site, 2 taxa (*P. pungens,* and *P. plurisecta*) were positively correlated with both temperature and salinity. *P. delicatissima,* Unknown 148, and Unknown 222/223 were negatively correlated with both temperature and salinity and Unknowns 155 and 187 were negatively correlated with temperature only. Positive correlations between 3 taxa (*P. multiseries, P. australis,* and *P. fraudulenta*) and salinity were revealed (Table 6). Analysis of both sites combined revealed positive correlations between 2 taxa (*P. pungens* and *P. plurisecta*) and both temperature and salinity. *P. delicatissima* and Unknowns 187 and 222/223 were negatively correlated with both temperature and salinity while *P.* sp. 147 and Unknowns 155 and 227/228 were negatively correlated with temperature only. *P. australis, P. seriata, P. americana,* and *P. fraudulenta* were positively correlated with salinity only (Table 7). At the Bar Harbor site, 4 taxa (*P. pungens, P. australis, P. seriata,* and *P. plurisecta*) were positively correlated with DA and 4 taxa (*P.* sp. 147, *P. delicatissima, P. cuspidata,* and Unknown 162) were negatively correlated with DA (Table 5). At MDIBL, 2 taxa (*P. pungens* and *P. australis*) were positively correlated with DA and 6 taxa (*P.* sp. 147, *P. delicatissima, P. cuspidata,* and Unknowns 148,187, 222/223) were negatively correlated with DA (Table 6).

Table 5. Spearman's rank correlation coefficient results for species versus temperature, salinity, domoic acid (pDA), and silicic acid (Si) at Bar Harbor. Only species with significant correlations are shown.

Species	Temperature	Salinity	pDA	Si
P. pungens	0.466	0.336	0.27	
P. sp. 147	-0.253		-0.239	
P. australis			0.448	
P. seriata	0.151	0.151	0.156	
Unknown 162 bp			-0.174	
P. delicatissima	-0.341	-0.235	-0.229	
P. fraudulenta	-0.161	0.198		
P. plurisecta	0.541		0.196	
Unknown 227/228 bp	-0.191			0.201
P. cuspidata			-0.166	

Table 6. Spearman's rank correlation coefficient results for species versus temperature, salinity, domoic acid (pDA), and silicic acid (Si) at MDIBL. Only species with significant correlations are shown.

Species	Temperature	Salinity	pDA	Si
P. pungens	0.425	0.271	0.328	
P. multiseries		0.153		
P. sp. 147			-0.31	
Unknown 148 bp	-0.209	-0.149	-0.195	
P. australis		0.33	0.571	
P. seriata				-0.173
Unknown 155 bp	-0.179			
P. delicatissima	-0.291	-0.34	-0.369	
Unknown 187 bp	-0.25		-0.247	
P. fraudulenta		0.166		
Unknown 217/218 bp				-0.171
Unknown 222/223 bp	-0.247	-0.209	-0.17	
P. plurisecta	0.385	0.209		
P. cuspidata			-0.319	

Table 7. Spearman's rank correlation coefficient results for species versus temperature, salinity, domoic acid (pDA), and silicic acid (Si) at Bar Harbor and MDIBL sites combined. Only species with significant correlations are shown.

Species	Temperature	Salinity	pDA	Si
P. pungens	0.421	0.306	0.295	
P. multiseries			0.151	
P. sp. 147	-0.122		-0.264	
Unknown 148 bp	-0.111	-0.119	-0.137	
P. australis		0.23	0.502	
P. seriata		0.13	0.146	
Unknown 155 bp	-0.124			
Unknown 162 bp			-0.121	
P. delicatissima	-0.316	-0.285	-0.28	
Unknown 187 bp	-0.157	-0.131	-0.197	
P. americana		0.13		-0.118
P. fraudulenta		0.188		
Unknown 222/223 bp	-0.149	-0.155	-0.121	
P. plurisecta	0.433	0.108	0.166	
Unknown 227/228 bp	-0.159			0.137
P. cuspidata			-0.245	

At the Bar Harbor site, 4 taxa (*P. pungens, P. australis, P. seriata,* and *P. plurisecta*) were positively correlated with DA and 4 taxa (*P.* sp. 147*, P. delicatissima, P. cuspidata,* and Unknown 162) were negatively correlated with DA (Table 5). At MDIBL, 2 taxa (*P. pungens* and *P. australis*) were positively correlated with DA and 6 taxa (*P.* sp. 147*, P. delicatissima, P. cuspidata,* and Unknowns 148,187, 222/223) were negatively correlated with DA (Table 6).

Analysis from both sites combined showed positive correlations between DA and 5 taxa (*P. pungens, P. multiseries, P. australis, P. seriata,* and *P. plurisecta*) and negative correlations between DA and 7 taxa (*P.* sp. 147*, P. delicatissima, P. cuspidata,* Unknowns 148, 162, 187, and 222/223) (Table 7). Combined sites also showed positive correlations between temperature and

taxa (*P. pungens* and *P. plurisecta*), and negative correlations between temperature and 7 taxa (P. sp. 147, *P. delicatissima,* Unknowns 148, 155, 187, and 227/228). Salinity was positively correlated with 6 taxa (*P. pungens, P. australis, P. seriata, P. americana, P. fraudulenta,* and *P. plurisecta*) and negatively correlated with 4 taxa (*P. delicatissima,* and Unknowns 148 and 222/223).

Statistical analysis – NMDS

Using the Bray-Curtis similarity matrix, nMDS showed distinct seasonal groupings across samples, despite some overlap (Figure 8). By adding species vector overlays to the nMDS, species that were significantly correlated with a particular season were highlighted (Figure 8A). In the spring, *P. delicatissima*, *P.* sp. 147, *P. cuspidata, P. americana,* Unknown 222/223, and Unknown 187 were dominant in (but not limited to) the spring; *P. plurisecta, P. seriata, P. pungens, P. fraudulenta* and *P. australis* were more dominant in the summer and fall. Winter samples did not ordinate closely, potentially due to the minimal and sporadic sampling conducted during these months. For example, there was only 1 sample collected in 2014 (December); 1 sample in 2015 (February); 4 samples collected in 2017 (December); 1 sample in 2020 (February); 4 samples in 2018 (December, January, February).

Environmental variable vectors show that temperature, salinity, and P have a higher correlation to species assemblages in the summer and fall samples and Si has higher correlation to assemblages in the spring (Figure 8). The pDA vector points more towards fall samples (with some summer overlap) which is when *P. australis* is most prevalent in 2016-2020 samples. NMDS ordinations across years showed a greater amount of overlap. However, years with *P. australis* presence and shellfish harvest closures (2016-2019) ordinated closer together with *P.*

australis being the longest vector and thus indicating the strong correlation between these years (Figure 9). Years without *P. australis* (2013-2015) were more correlated with *P. plurisecta, P. fraudulenta, P. seriata,* and *P. pungens* as indicated by the direction and magnitude of vectors (Figure 9). In 2020, samples were more widespread than other *P. australis* years (2016-2020); as previously mentioned, *P. australis* was present in 2020 but there were no shellfish harvest closures in Maine. By adding environmental vectors to the nMDS plot, Si is correlated with points towards the left of the plot whereas temperature, salinity, P, and pDA vectors influence data towards the right (Figure 9).

Statistical analysis – ANOSIM of species and environmental data

ANOSIM was used to quantify these annual and seasonal differences among species assemblages. There were some significant differences across years but some overlap was observed across years and the degree to which they differ is minimal. Years 2014 and 2019 were the most similar to each other and there was no significant difference in species assemblages ($R=0.025$; $p>0.05$). 2014 and 2018 were the most significantly different years ($R=0.387$; $p<0.05$). For seasonal comparisons, the fall season was the most different season compared to spring, winter, and summer. Fall and spring seasons were the most different from each other ($R=0.718$; $p<0.05$), fall and winter were the second most different ($R=0.514$; $p<0.05$) and fall versus summer was the third most different ($R=0.22$; $p<0.05$). Summer and winter comparison showed that these seasons were the least different from each other ($R=0.127$; $p<0.05$), likely due to lower sampling in winter ($n=12$) compared to summer ($n=185$) and the presence of *P. delicatissima* in both of these seasons.

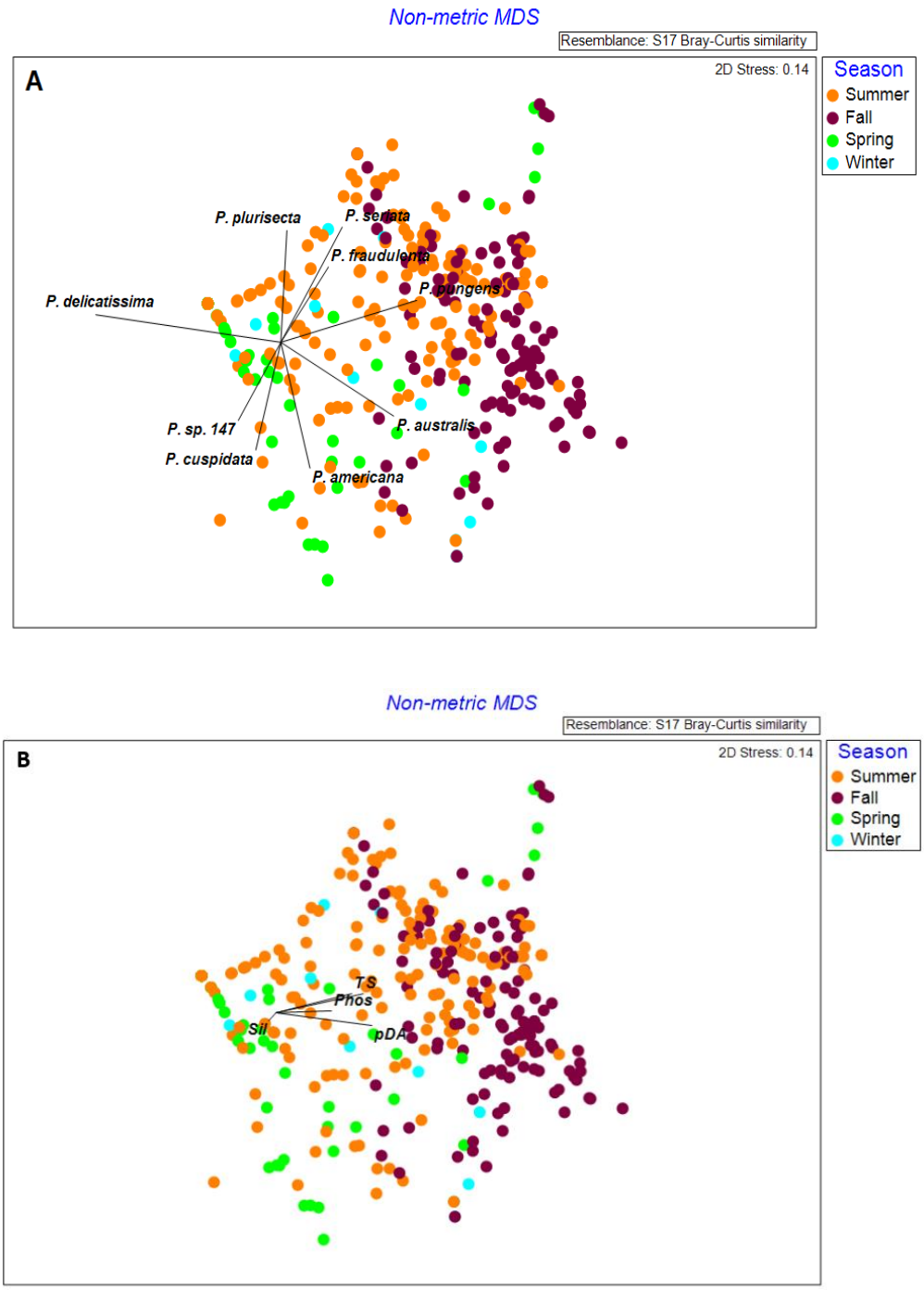

Figure 8. NMDS ordinations grouped by season. The distance between sample points on the plots indicates the similarity in species composition, with closer points being more similar. Vectors representing species (A) or environmental variables (B) were superimposed on the nMDS plots to indicate the direction in which the variable is increasing. The length of the vector represents the magnitude of the correlation between the variable and species composition.

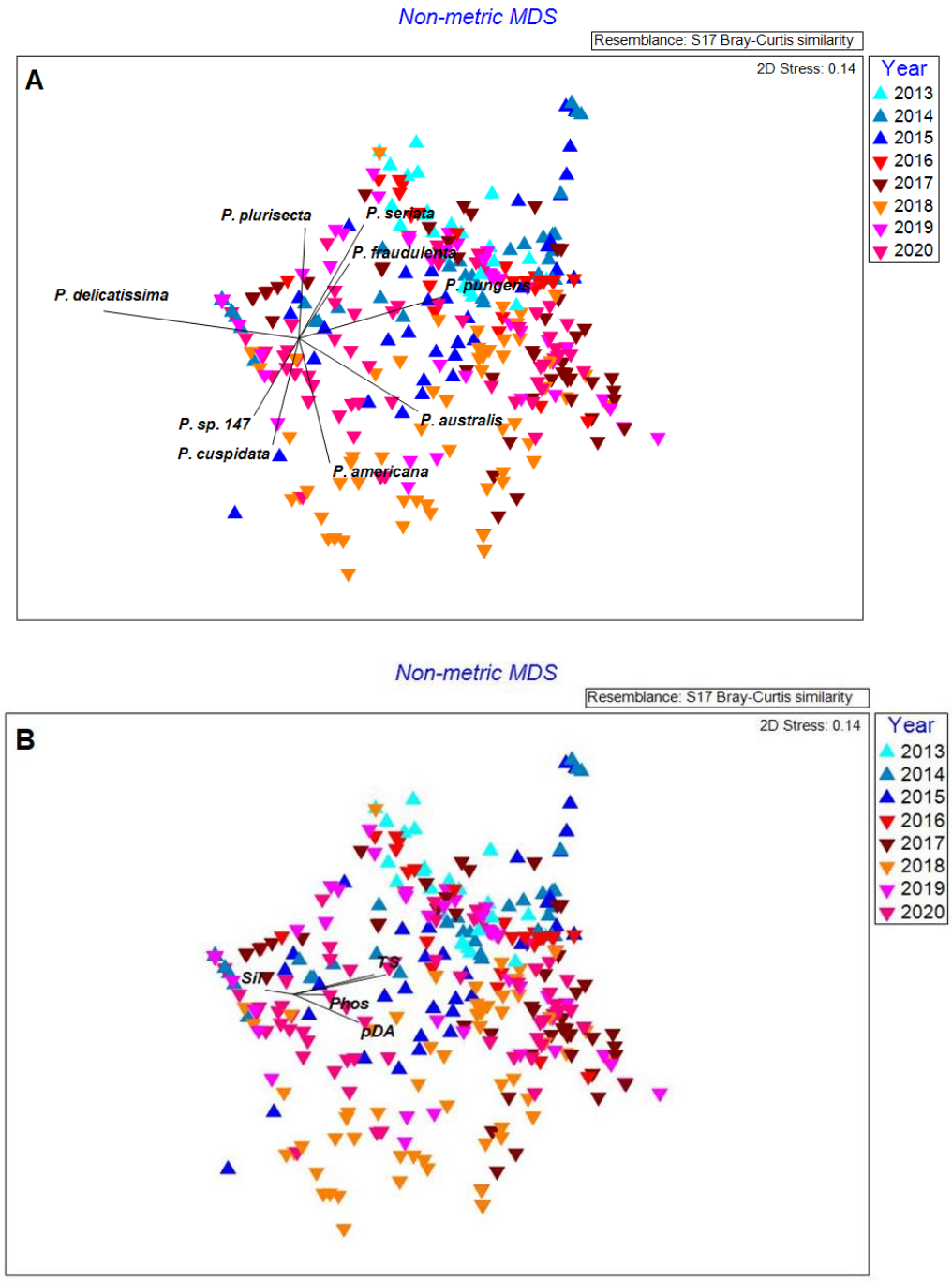

Figure 9. NMDS ordinations grouped by year. The distance between sample points on the plots indicates the similarity (or dissimilarity) in species composition. Vectors representing species (A) or environmental variables (B) were superimposed on the nMDS plots to indicate the direction of which the variable is increasing. The length of the vector represents the magnitude of the correlation between the variable and species composition.

ANOSIM results for the full environmental dataset across years revealed that 2015 and 2020 were the most different ($R=0.347$, $p<0.05$); 2015 and 2018 were the second most different ($R=0.295$; $p<0.05$); 2013 and 2015 were the third most different ($R=0.281$; $p<0.05$).2014 and 2019 environmental data were the most similar ($R=0.041$; $p<0.05$) which matches results from the species data. ANOSIM results for the partial environmental dataset (2013-2017) showed that 2013 and 2015 environmental data were the most different ($R=0.265$; $p<0.05$) and 2013 and 2016 were the most similar ($R=0.084$; $p<0.05$). It is important to keep in mind that sample coverage varied across seasons and years.

Statistical analysis – BVSTEP (BIOENV) and PCA

To test which species best represented a season, BVSTEP (step-wise BIOENV) in the BEST function in PRIMER was run for each season individually. The species with the highest correlation to spring (in order of strongest correlation) were *P. delicatissima* and *P. cuspidata* ($R=0.97$; $p<0.05$). Species correlated with summer were *P. pungens, P. delicatissima, P. plurisecta,* and *P. cuspidata* ($R=0.951$; $p<0.05$). *P. australis, P. pungens, P. plurisecta,* and *P. americana* ($R=0.97$; $p<0.05$) were correlated with fall. Species correlated with winter were *P. americana, P. delicatissima,* and *P. pungens* ($R=0.97$; $p<0.05$).

PCA was conducted on the full environmental dataset with all variables (temperature, salinity, DA, nutrients, and nutrient ratios) included and showed that temperature, salinity, Si, P, and NO_x made up the largest percentages of variation between samples; temperature (34.9%), salinity (21.1%), Si (16.2%), P (9.7%) and NO_x^- (6.1%). Cumulative variation revealed that temperature and salinity together accounted for 56.1% of variation in samples; temperature, salinity, and Si accounted for 72.3% of variation; temperature, salinity, Si, and P accounted for

82% of variation; temperature, salinity, Si, P, and NO_x accounted for 88.1% of variation. This indicates that the combination of certain environmental factors has more influence on the variability as opposed to the individual factors.

Summer-fall seasonal observations: Temperature, salinity, Si, and pDA

Evidence provided by the descriptive and statistical analyses, the summer-fall seasons have the highest *Pseudo-nitzschia* cell abundances (Figure 2, Table 2), increased pDA (Figure 7), and prevalence of multiple toxin-producing *Pseudo-nitzschia* species compared to all other seasons (Figures 4 and 5). Patterns among temperature, salinity, cumulative upwelling indices (CUI), Si, and pDA in the summer-fall seasons were examined further in an attempt to highlight important underlying processes that may be driving species assemblages and toxicity in this timeframe.

The results from the offshore NERACOOS Buoy I (Figure 10) revealed interannual and seasonal trends in temperature and salinity. Buoy data from 2017 were not available therefore offshore temperature and salinity comparisons are for 2013-2016, 2018-2020. Past research has shown that 2016 had the warmest offshore temperatures in summer and fall seasons compared to preceding years (2013-2015) (Clark et al., 2019). 2016 had warmer monthly means from June-November compared to 2013-2015, except for October 2014, where the temperature mean was approximately the same as October 2016. 2016 summer season was 2 °C warmer and fall was 1 °C warmer than 2013-2015. 2016 had the highest monthly mean temperatures for years succeeding (2018-2020) except for August which was the highest in 2018 (Figure 10). In all years, temperature increased from June-August and began to decrease in September except for 2016 which had the same temperature from August-September. Fall 2016 and 2018 were warmer

than 2015 and the mean fall offshore temperature differed very little between 2015, 2019, and 2020. Between June and July, temperature increased 2.4 °C in 2016 and 3.0 °C in 2019. Temperature further increased from July to August by 1.2 °C in 2016 and 0.9 °C in 2019. From August-September, temperature decreased slightly or remained around the same temperature and larger decreases in temperature were observed from September to October. *P. australis* blooms were initiated roughly around the same time of year (September 26th in 2016 and September 24th in 2019). In 2018, temperature had an earlier increase of 2.8 °C from June-July and another 2.1 °C temperature increase from July-August and the *P. australis* bloom initiated earlier on September 6th. In 2020, there was a 1.9 °C temperature increase from June-July and another 1.9 °C increase from July-August and the *P. australis* bloom began on August 26th.

In all years, salinity increased from summer to fall (Figure 10). July 2016 was anomalously saline offshore compared to previous years (Clark et al., 2019) and compared to succeeding years (2018-2019) – however, no offshore salinity data was available for 2017 or 2020. Salinity in 2018 June-July was roughly the same as salinity means in 2016. Salinity in fall 2016 was roughly the same as salinities in the 2015 and 2018 fall seasons. Salinity in September-November was highest in 2014 (Figure 10). The results from inshore sampling at the two sites revealed trends among temperature, salinity, and species composition. Inshore temperatures from October-November typically decreased by 1.1-2.9 °C, except for in 2017 where temperature only decreased 0.4 °C from October-November (Figure 10). The 2017 *P. australis* bloom occurred the earliest (Figure 6) and lasted the longest compared to all other years and was associated with a temperature increase of 3.2 °C from June-July; *P. australis* began blooming on August 9th and persisted through the winter. Mean inshore temperatures in 2013, 2014, and 2020 were higher in June compared to all years (Figure 10). 2018 had the highest monthly mean temperatures for

July-September. Like the offshore mean temperature, the October inshore mean temperature was the highest in October 2016. July inshore salinity was also the highest in 2016. 2017-2019 inshore salinities were lowest in July and August compared to preceding years. Overall, 2020 had the highest monthly average salinities for June, August, September, October, and November and closely resembled the salinities observed in 2013 (Figure 10).

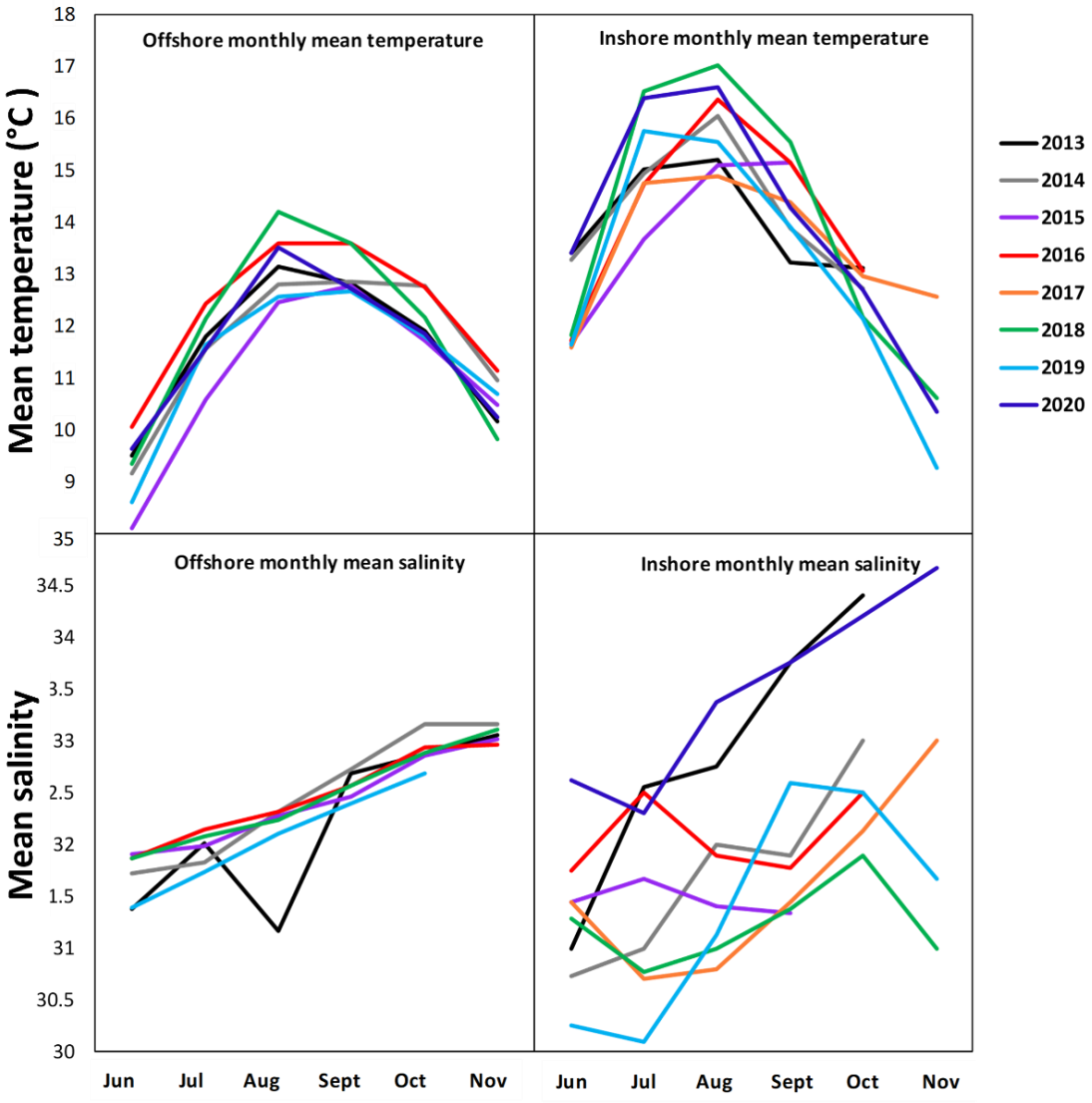

Figure 10. Monthly average temperature and salinity from June-November in 2013-2020 obtained from offshore NERACOOS Buoy I and inshore sampling (Bar Harbor and MDIBL sites).

Mean Si concentrations at both sites in July 2016 were the highest compared to all other years and a gradual decline in concentration was observed from July-September. Inversely, 2017 had anomalously low mean Si concentrations in July and August at both sites and showed a gradual increase in concentration from July-September. 2013, 2015, 2019, and 2020 mean Si concentrations showed an increase from July-August then a decrease from August-September. Inversely, 2014 and 2018 showed a decrease from July-August then an increase from August-September. 2020 had the highest mean Si concentrations in August and September compared to all other years. Mean Si concentrations were typically higher at the MDIBL site than the Bar Harbor site, likely due to the proximity of riverine outflows.

Focusing only on the July-September timeframe, the highest pDA concentrations in September were observed in 2017 at both sites (Figure 7). The second highest concentrations were observed in July and August 2013, concurrent with a *P. plurisecta* bloom that occurred in that summer. Then, toxin concentrations decreased drastically from August-September in 2013. Aside from 2013, gradual increases in pDA concentration were typically observed from July-August and from August-September, except in 2014 and 2020 where there was a slight decrease in pDA concentrations from August-September. Peak pDA concentrations occurred in October for 2019-2020.

NERACOOS Buoy I CUI data contains data from 2013-2018. Clark et al. (2019) highlights that the summer CUI in 2016 had a more rapid increase than 2013-2015 and that a shift to downwelling winds occurred from September 23rd-27th. *P. australis* was first observed and persisted at the Bar Harbor and MDIBL sites just before the shift to downwelling-favorable winds (Figure 11). CUI in June 2017 was greater than in 2016 but lower in July 2017. *P.*

australis was first observed at the end of July and persisted approximately 1 week later in August. In 2017, a rapid increase was observed at the end of August leading into the 1st week of September where CUI was higher than during this timeframe in 2016 (Figure 11). Conditions relaxed from September 9th-19th where there was a period of no change. Then a shift to downwelling-favorable conditions occurred on September 20th. 2018 CUI follows similar trends as 2016 until August 20th, where it tapers off and does not have rapid increases. Alternating shifts from upwelling-favorable to downwelling-favorable winds occur approximately weekly from September through October in 2018. *P. australis* was observed sporadically in samples this year in March, April, May, and June but did not persist until early September (Figure 11). Overall, there is a general increase in upwelling in the summer and more variability in the fall where there are alternations between upwelling-favorable to downwelling-favorable conditions.

Examining trends from the 2017 *P. australis* bloom

Since 2017 had the highest *Pseudo-nitzschia* cell abundance, high levels of pDA, longest shellfish toxicity above the regulatory limit, and longest persistence of *P. australis* recorded, this year was selected to highlight temporal trends in species composition, temperature, salinity, Si, DA, and CUI in the summer-fall timeframe (Figure 12). *P. plurisecta* was first observed at both sites on July 3rd; *P. pungens* joined the assemblage on July 18th in MDIBL and August 1st in Bar Harbor; *P. seriata* joined the assemblage on July 24th at both sites; *P. australis* became part of the assemblage on August 9th in MDIBL and August 20th in Bar Harbor (Figure 12).

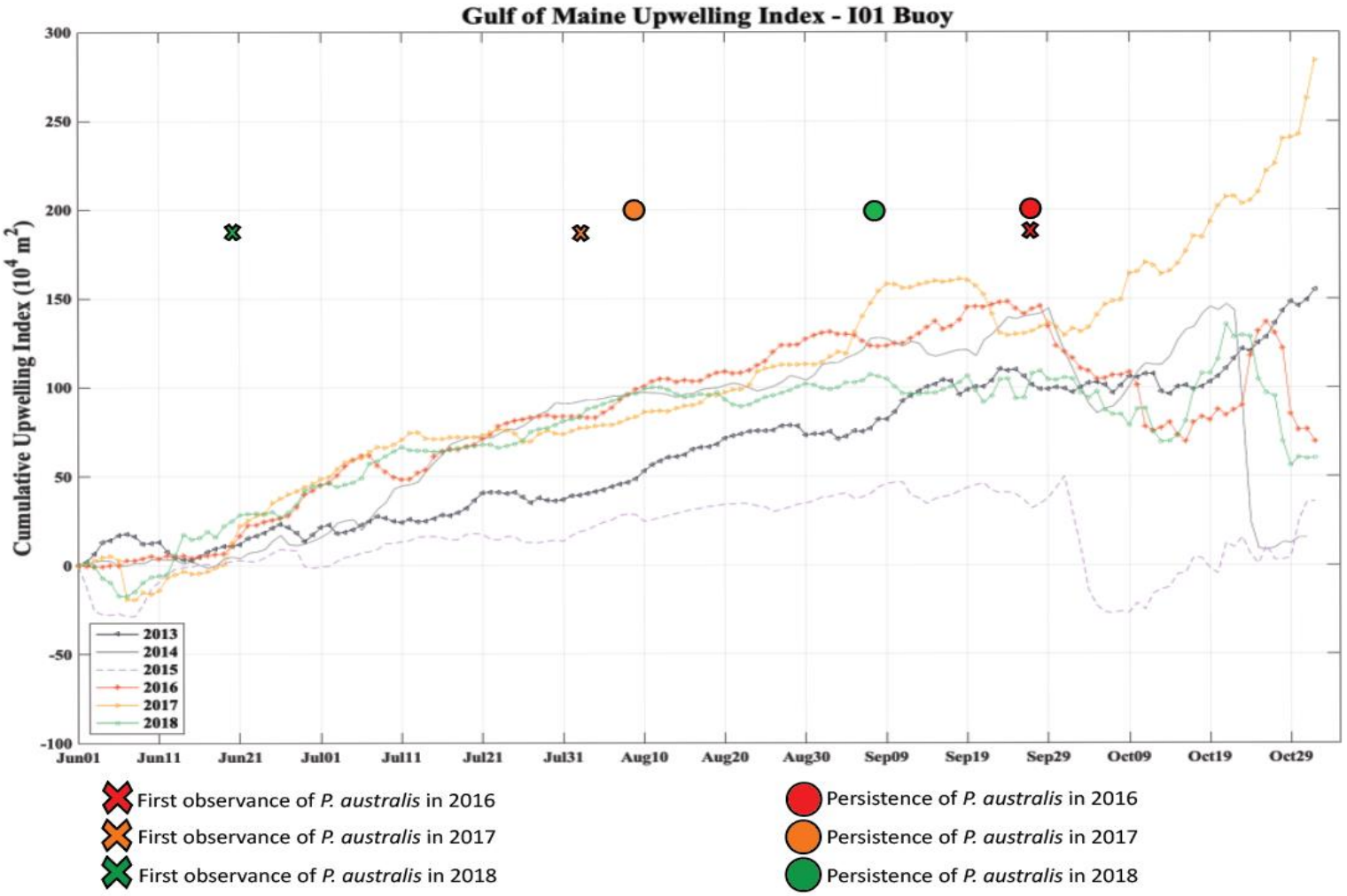

Figure 11. Cumulative upwelling indices in 2013-2018 using data obtained from NERACOOS Buoy I. Dates of first observance and persistence (defined as lasting more than 2 consecutive weeks) of *P. australis* in 2016-2018 are shown in crosses and circles, respectively.

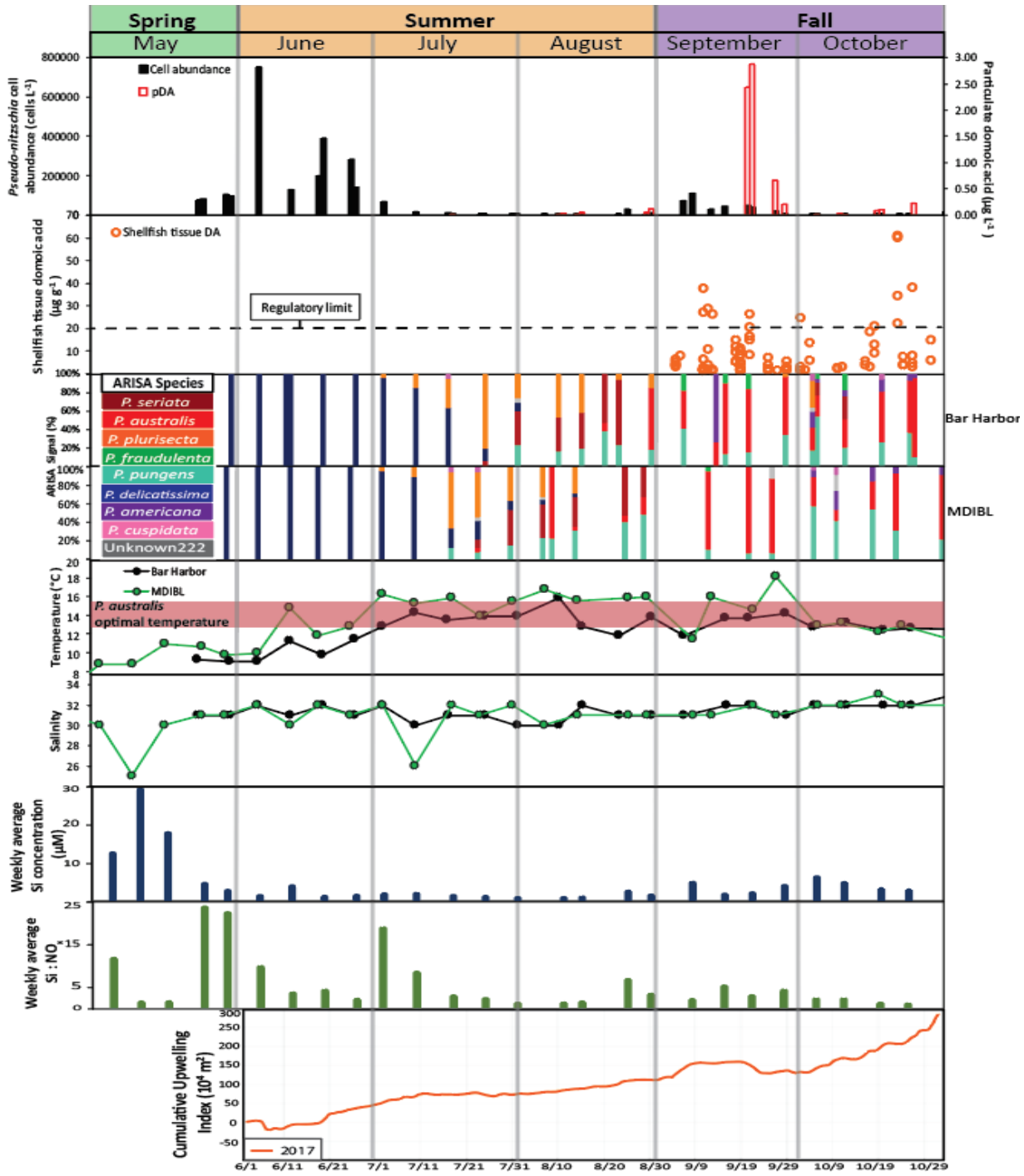

Figure 12. *Pseudo-nitzschia* species, domoic acid, and environmental data from May-October, 2017. Cell abundance and pDA data were plotted on the same axis and represent both sites combined. Si, Si:NO_x ratio weekly averages were calculated using both sites combined data. Temperature and salinity data were obtained from the Bar Harbor and MDIBL sites. CUI was calculated using data obtained from NERACOOS Buoy I.

Average inshore temperatures were 11.6 °C in June, 14.8 °C in July, 14.9 °C in August, 14.4 °C in September, and 13 °C in October. Salinity decreased from June-July but increased from July-August and a greater increase was observed from August-September. The highest increases in pDA were observed from August-September where there was an average pDA of 1.2 µg L^{-1} in Bar Harbor and 1.7 µg L^{-1} in MDIBL. DA was first detected in shellfish on September 4th and surpassed the regulatory limit (20 µg DA g^{-1} shellfish tissue) on September 10th. Toxin levels remained above the regulatory limit through December at some sites (Figure 12).

Average Si concentrations increased by 1.6 µM in Bar Harbor and 2 µM in MDIBL from August-September. Si:NO_x ratio was the highest in July and decreased drastically in August at both sites (Figure 12). CUI increased in July, switched to downwelling-favorable winds between July 21st and July 31st, then reverted back to upwelling-favorable winds in August. A rapid increase in CUI was observed between August 31st and September 9th and then stabilized from September 9th through September 19th. CUI began to decrease on September 19th followed by another period of relaxed winds before another period of upwelling-favorable conditions. At the end of September and into October, CUI increased followed by a period of relaxed winds, and this pattern repeated through the end of October.

Conceptual bloom model

To better understand the sequence of events during a bloom, a conceptual bloom model was formed after analyzing the 2013-2020 *Pseudo-nitzschia* blooms (Figure 13). This conceptual model highlights the sequence of events however it is important to note that the months at which a change in the system occurred varied across years. Despite some variability, the sequence of changes observed were similar across years. In general, upwelling occurred in the summer and

became more variable in the fall where shifts between upwelling and downwelling were observed. Si concentrations were high in mid spring and high *Pseudo-nitzschia* cell abundance was observed in late spring and summer months. In the summer, *P. plurisecta* was observed and was associated with low levels of pDA concurrent with warming temperatures. In the late summer, lower levels of Si concentrations were observed. In the fall, lower *Pseudo-nitzschia* cell abundance was observed and this is typically when *P. australis* joined the species assemblage and was associated with high levels of pDA. In the mid fall, low Si:NO_x ratio was typically observed.

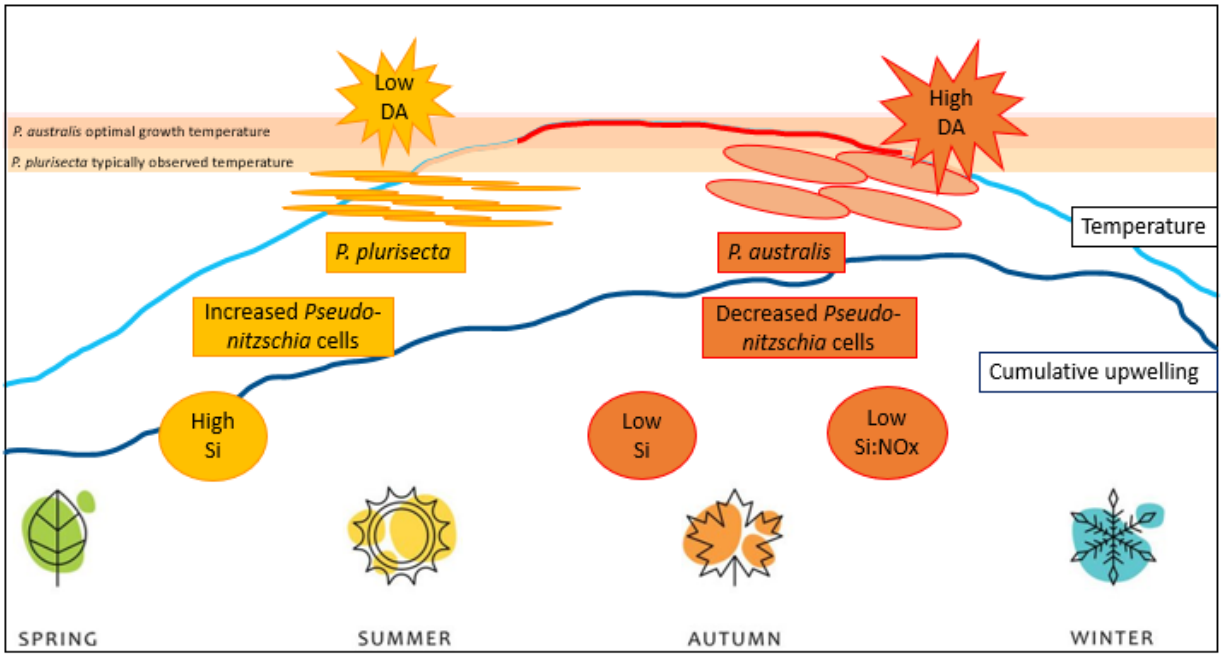

Figure 13. Conceptual bloom model highlighting the typical sequence of events during a bloom. This model was built from analysis of patterns in blooms from 2013-2020.

Discussion

Pseudo-nitzschia species composition and domoic acid

This study highlighted seasonal and episodic trends in *Pseudo-nitzschia* species composition, environmental, hydrodynamic, and nutrient conditions in the Gulf of Maine during 2013-2020. Shifts were observed during the fall months of August-September where *P. pungens, P. plurisecta,* and *P. seriata* were the dominant species in the assemblage and shifted to include *P. australis* in 2016-2020. Another compositional shift was observed in 2016-2020 after the *P. australis* peak when the late fall assemblage primarily consisted of *P. americana*. In the years preceding *P. australis,* the typical late fall assemblage usually consisted of *P. seriata, P. pungens,* and *P. fraudulenta.* One caveat is that there is higher sample resolution for 2017-2020 than preceding years, particularly in the winter (December, January, February) and spring months (March, April, May) and some *P. americana* presence may have been missed in 2013-2016 winter months due to reduced sampling. Regardless, there is still a larger *P. americana* presence in the late fall (October-November) months in 2017-2020 compared to 2013-2014. Another notable compositional shift that was observed is that *P. seriata* dominated in fall months in the years preceding *P. australis* but was seen in relatively low proportions in years succeeding the observance of *P. australis.*

Species composition affects DA production and concentrations of pDA depend on both the abundance and diversity of *Pseudo-nitzschia* species (Thorel et al., 2017). Past research has revealed that higher DA concentrations corresponded to communities dominated by toxic *P. australis/P. seriata* species and lower DA concentrations were observed when there was a mixed assemblage of *P. cuspidata* and *P. heimii/P. americana* (Smith et al., 2018). In this thesis, the

highest pDA concentrations were observed when multiple toxic species (*P. plurisecta, P. seriata, P. australis,* and *P. pungens*) were present concurrently. The production of DA by *Pseudo-nitzschia* species may improve the competitive ability of this genus (Prince et al., 2013). Dissolved DA (dDA) in the water column coupled with increased salinity has been shown to inhibit the growth of certain phytoplankton species (Van Meerssche and Pinckney, 2017) thus providing a potential competitive advantage of *Pseudo-nitzschia* species over other organisms, particularly under iron-replete conditions (Prince et al., 2013).

An interesting finding from this thesis was the apparent disconnect between shellfish toxicity and particulate DA from seawater. The decline in shellfish toxicity from 2016-2020 contrasted with the highest pDA observations (2017 at Bar Harbor and 2019 at MDIBL). Potential mechanisms driving the steady decline in shellfish toxicity may be oceanic circulation, stage of sexual reproduction that *P. australis* was in, nutrient availability and stoichiometry, changes in vertical structure of the water column, changes in grazing, and duration of the bloom (Figures 4 and 5). One caveat to comparing the pDA and shellfish DA is that pDA does not account for any dissolved DA in seawater and is only the DA measured within the phytoplankton. It should also be noted that shellfish DA samples had larger spatial coverage spanning the entire Maine coast whereas the pDA data was only collected at the Bar Harbor and MDIBL sites, approximately at the midpoint of the Maine coast. However, the shellfish DA data from the Bar Harbor site was analyzed separately and the same overall downward trend in toxicity over time as seen with all shellfish sites combined was observed.

Temperature, nutrients, and upwelling

Recent laboratory observations of a *P. australis* culture isolated from the MDIBL site revealed that the optimal growth temperature for this species is between approximately 13 °C-15 °C (Clark et al., 2021). Optimal temperature for another isolate of *P. australis* was shown to be between 13.6 °C -18.6 °C depending on varying levels of irradiance (Thorel et al., 2014). Field observations from this study show that *P. australis* was observed in average inshore temperatures across years ranging from 13.9 °C-16.4 °C, indicating temperature as an important factor for changes in species composition and pDA production.

Focusing on the 2017 bloom, *P. australis* may have persisted the longest in this year because of the sustained high temperatures in October and November around 13 °C. Compared to other years with *P. australis*, temperature usually decreased in October and decreased again in November. The 2017 bloom was also accompanied by periods of upwelling-favorable conditions followed by periods of relaxed winds from August-September which has been shown to favor diatom growth (Wilkerson et al., 2006). The large increase in *Pseudo-nitzschia* cellular abundance observed at the end of May through the end of June may be due to the rapid uptake of Si from upwelled nutrients to support high *Pseudo-nitzschia* cellular growth in this year. This rapid uptake of Si supports the dramatic decrease in Si:NO_x that was later observed from July-August. A lower Si:NO_x ratio during the July-August time period may have arrested cellular growth and supported the pDA production which began at the end of August and peaked in September. Therefore, temperature, presence of multiple toxic species, and timing of nutrient availability were driving forces for this vastly toxic *P. australis* bloom in 2017. This combination has been supported by other studies, specifically in the 2015 Monterey Bay *P. australis* bloom

which was initiated by upwelled nutrients followed by cessation of upwelling and warmer temperatures (McCabe et al., 2016). Similarly, the occurrence of multiple toxic species and higher pDA concentrations was observed when Si concentrations decreased towards the end of an upwelling event in California (Smith et al., 2018).

Future research

Other molecular methods should be explored to enhance the findings of this thesis. The ARISA method is unable to quantify the cellular abundances of a particular *Pseudo-nitzschia* species and electron microscopy methods are time-consuming and require a high level of taxonomic training to complete. Quantitative PCR (qPCR) would be a suitable method for quantifying the abundances of specific toxigenic species and may reveal patterns in species composition that are not yet characterized. Targeted sequencing of some of the "Unknown" size fragments from the ARISA method should also be conducted to potentially identify novel *Pseudo-nitzschia* species in the Gulf of Maine.

Continued monitoring of *Pseudo-nitzschia* species assemblages and changes in environmental conditions in the Gulf of Maine will improve our understanding of the underlying dynamics of this HAB-forming genus. While several trends in species composition, toxicity, and environmental patterns were highlighted here, a longer time series containing more years of sampling will help solidify theorized drivers of blooms and toxicity and may reveal drivers that have not yet been discovered. A longer time series will also contribute to future modeling projections to enhance bloom forecasting efforts. Recent modeling efforts projected changes in *Pseudo-nitzschia* dynamics in the Gulf of Maine due to elevated temperature, decreased salinity, and increased stratification resulting from global climate change (Clark et al., 2022). Since *P.*

australis has been shown to have a relatively specific optimal temperature range (average field observations from this thesis ranged from 13.9 °C-16.4 °C) these projected temperature changes may alter the growth, timing, and spatial preferences of this toxigenic species (Clark et al., 2022). Thus, it is predicted that an overall shift in *Pseudo-nitzschia* species assemblages may occur due to effects of climate change (Clark et al., 2022). Including more field data observations will lend more information for future modeling work and improve our understanding of the effects of climate change on *Pseudo-nitzschia* bloom dynamics in the Gulf of Maine.

Conclusion

This thesis successfully addressed each proposed hypothesis and revealed trends in *Pseudo-nitzschia* species composition, DA, and environmental variables that vary at event, seasonal, and annual time scales. In general, we observed similar species assemblages in 2013-2014, novel diversity in 2015, and the introduction of a particularly toxic species in 2016 that persisted through the duration of the study. Given these differences, species assemblages varied across seasons but seasons across years shared similar diversity. Two toxic species, *P. plurisecta* and *P. australis,* generally were associated with toxicity in summer and fall, respectively. However, fall assemblages coincident with *P. australis* tended to be the most toxic. Furthermore, peak toxicity associated with *P. australis* varied across years and particulate DA concentrations did not always track with shellfish toxicity, suggesting that additional mechanisms may contribute to the severity of impacts.

The results from this study enabled conceptualization of *Pseudo-nitzschia* species dynamics and the underlying factors controlling bloom events. The timing of the changes of

bloom drivers is important for the timing and severity of bloom events. Results support that inshore and offshore processes are connected and there is likely a time lag between changes in offshore processes (such as upwelling) and its effect on inshore processes, suggesting that offshore processes are important for estuarine patterns observed in this study. Characterizing species composition, DA, and environmental variables in the GOM across years highlighted anomalies (such as the introduction of *P. australis* to the system) and enabled the identification of regime shifts. The findings in this study will enhance our understanding of how the GOM system will respond to future anomalous events (such as introduction of other novel species or changes in ocean temperature) and will strengthen ongoing forecasting and monitoring efforts of *Pseudo-nitzschia* blooms in the GOM.

REFERENCES

Ajani, P. A., Verma, A., Lassudrie, M., Doblin, M. A., & Murray, S. A. (2018). A new diatom species *P. hallegraeffii* sp. nov. belonging to the toxic genus *Pseudo-nitzschia* (Bacillariophyceae) from the East Australian Current. *PloS One, 13*(4), e0195622.

Amato, A., Kooistra, W. H., Ghiron, J. H. L., Mann, D. G., Pröschold, T., & Montresor, M. (2007). Reproductive isolation among sympatric cryptic species in marine diatoms. *Protist*, *158*(2), 193-207.

Anderson, C. R., Brzezinski, M. A., Washburn, L., & Kudela, R. (2006). Circulation and environmental conditions during a toxigenic *Pseudo-nitzschia australis* bloom in the Santa Barbara Channel, California. *Marine Ecology Progress Series*, *327*, 119-133.

Anderson, D. M. (2009). Approaches to monitoring, control and management of harmful algal blooms (HABs). *Ocean & Coastal management*, *52*(7), 342-347.

Anderson, D. M., Kulis, D. M., Sullivan, J. J., Hall, S., & Lee, C. (1990). Dynamics and physiology of saxitoxin production by the dinoflagellates *Alexandrium* spp. *Marine Biology*, *104*(3), 511-524.

Auro, M. E. (2007). Nitrogen dynamics and toxicity of the pennate diatom *Pseudo-nitzschia cuspidata*: A field and laboratory based study (Doctoral dissertation, San Francisco State University).

Auro, M. E., & Cochlan, W. P. (2013). Nitrogen utilization and toxin production by two diatoms of the *Pseudo-nitzschia pseudodelicatissima* complex: *P. cuspidata and P. fryxelliana. Journal of Phycology*, *49*(1), 156-169.

Ayache, N., Hervé, F., Lundholm, N., Amzil, Z., & Caruana, A. M. (2020). Acclimation of the marine diatom *Pseudo-nitzschia australis* to different salinity conditions: Effects on growth, photosynthetic activity, and domoic acid content. *Journal of Phycology*, *56*(1), 97-109.

Bargu, S., Powell, C. L., Coale, S. L., Busman, M., Doucette, G. J., & Silver, M. W. (2002). Krill: a potential vector for domoic acid in marine food webs. *Marine Ecology Progress Series*, *237*, 209-216.

Bates, S. S., Bird, C. J., Freitas, A. D., Foxall, R., Gilgan, M., Hanic, L. A., ... & Wright, J. L. C. (1989). Pennate diatom *Nitzschia pungens* as the primary source of domoic acid, a toxin in shellfish from eastern Prince Edward Island, Canada. *Canadian Journal of Fisheries and Aquatic Sciences*, *46*(7), 1203-1215.

Bates, S. S., Freitas, A. D., Milley, J. E., Pocklington, R., Quilliam, M. A., Smith, J. C., & Worms, J. (1991). Controls on domoic acid production by the diatom *Nitzschia pungens* f. *multiseries* in culture: nutrients and irradiance. *Canadian Journal of Fisheries and Aquatic Sciences*, *48*(7), 1136-1144.

Bates, S. S. (1998) (A). Ecophysiology and metabolism of ASP toxin production. *NATO ASI series G Ecological Sciences*, *41*, 405-426.

Bates, S. S., Garrison, D. L., & Horner, R. A. (1998) (B). Bloom dynamics and physiology of domoic-acid-producing Pseudo-nitzschia species. *NATO ASI series G Ecological Sciences*, *41*, 267-292.

Bates, S. S., Hubbard, K. A., Lundholm, N., Montresor, M., & Leaw, C. P. (2018). *Pseudo-nitzschia*, *Nitzschia*, and domoic acid: new research since 2011. *Harmful Algae*, *79*, 3-43.

Bates, S. S., Léger, C., Satchwell, M., & Boyer, G. L. (2000). The effects of iron on domoic acid production by *Pseudo-nitzschia multiseries*. *Harmful Algal Blooms*, 320-323.

Berger, W. H., Smetacek, V. S., & Wefer, G. (1989). Ocean productivity and paleoproductivity—an overview. *Productivity of the Ocean: Present and Past*, *44*, 1-34.

Bigelow, H. B., Lillick, L. C., & Sears, M. (1940). Phytoplankton and planktonic protozoa of the offshore waters of the Gulf of Maine. *Transactions of the American Philosophical Society*, *31*(3), 149-237.

Bornet, B., Antoine, E., Françoise, S., & Baut, C. M. L. (2005). Development of sequence characterized amplified region markers from intersimple sequence repeat fingerprints for the molecular detection of toxic phytoplankton *Alexandrium catenella* (Dinophyceae) and *Pseudo-nitzschia pseudodelicatissima* (Bacillariophyceae) from French coastal waters. *Journal of Phycology, 41(3),* 704-711.

Brooks, D. A., & Townsend, D. W. (1989). Variability of the coastal current and nutrient pathways in the eastern Gulf of Maine. *Journal of Marine Research*, *47*(2), 303-321.

Burns, J. M., & Ferry, J. L. (2007). Adsorption of domoic acid to marine sediments and clays. *Journal of Environmental Monitoring, 9(12)*, 1373-1377

Burson, A., Stomp, M., Greenwell, E., Grosse, J., & Huisman, J. (2018). Competition for nutrients and light: testing advances in resource competition with a natural phytoplankton community. *Ecology*, *99*(5), 1108-1118.

Cavender-Bares, K. K., Karl, D. M., & Chisholm, S. W. (2001). Nutrient gradients in the western North Atlantic Ocean: Relationship to microbial community structure and comparison to patterns in the Pacific Ocean. *Deep Sea Research Part I: Oceanographic Research Papers*, *48(11)*, 2373-2395.

Chen, X. M., Pang, J. X., Huang, C. X., Lundholm, N., Teng, S. T., Li, A., & Li, Y. (2021). Two new and nontoxigenic *Pseudo-nitzschia species* (Bacillariophyceae) from Chinese Southeast coastal waters. *Journal of Phycology*, *57*(1), 335-344.

Clark, S., Hubbard, K. A., Anderson, D. M., McGillicuddy Jr, D. J., Ralston, D. K., & Townsend, D. W. (2019). *Pseudo-nitzschia* bloom dynamics in the Gulf of Maine: 2012–2016. *Harmful Algae*, *88*, 101656.

Clark, S., Hubbard, K. A., McGillicuddy Jr, D. J., Ralston, D. K., & Shankar, S. (2021). Investigating *Pseudo-nitzschia* australis introduction to the Gulf of Maine with observations and models. *Continental Shelf Research*, *228*, 104493.

Clark, S., Hubbard, K. A., Ralston, D. K., McGillicuddy Jr, D. J., Stock, C., Alexander, M. A., & Curchitser, E. (2022). Projected effects of climate change on *Pseudo-nitzschia* bloom dynamics in the Gulf of Maine. *Journal of Marine Systems*, *230*, 103737.

Darley, W. M., & Volcani, B. E. (1969). Role of silicon in diatom metabolism: a silicon requirement for deoxyribonucleic acid synthesis in the diatom *Cylindrotheca fusiformis* Reimann and Lewin. *Experimental Cell Research*, *58*(2-3), 334-342.

Dewar, D. (1989). Identification of domoic acid, a neuroexcitatory amino acid, in toxic mussels from eastern Prince Edward Island. *Canadian Journal of Chemistry*, *67*(3), 481-490.

Doan-Nhu, H., NGUYEN, T., & Nguyen-Ngoc, T. G. (2008). Pseudo-nitzschia in south-central coastal waters of Vietnam: growth and occurrence related to temperature and salinity. In *Proceedings of the 12th International Conference on Harmful Algae (Ed. by Ø. Moestrup)*, 29-32.

Dong, H. C., Lundholm, N., Teng, S. T., Li, A., Wang, C., Hu, Y., & Li, Y. (2020). Occurrence of *Pseudo-nitzschia* species and associated domoic acid production along the Guangdong coast, South China Sea. *Harmful Algae*, *98*, 101899.

Doucette, G. J., King, K. L., Thessen, A. E., & Dortch, Q. (2008). The effect of salinity on domoic acid production by the diatom *Pseudo-nitzschia multiseries*. *Nova Hedwigia*, *133*(31), 1439-0485.

Du, X., Peterson, W., Fisher, J., Hunter, M., & Peterson, J. (2016). Initiation and development of a toxic and persistent *Pseudo-nitzschia* bloom off the Oregon coast in spring/summer 2015. *PLoS One*, *11*(10), e0163977.

Falkowski, P. G. (1994). The role of phytoplankton photosynthesis in global biogeochemical cycles. *Photosynthesis Research*, *39*, 235-258.

Martin, J. H., Falkowski, P. G., & Woodhead, A. D. (1992). Primary productivity and biogeochemical cycles in the sea. *Edited by PG Falkowski, AD Woodhead*, 123.

Falkowski, P. G., & Woodhead, A. D. (Eds.). (2013). *Primary productivity and biogeochemical cycles in the sea* (Vol. 43). Springer Science & Business Media.

Fehling, J., Davidson, K., & Bates, S. S. (2005). Growth dynamics of non-toxic *Pseudo-nitzschia* delicatissima and toxic *P. seriata* (Bacillariophyceae) under simulated spring and summer photoperiods. *Harmful Algae*, *4*(4), 763-769.

Fehling, J., Green, D. H., Davidson, K., Bolch, C. J., & Bates, S. S. (2004). Domoic acid production by *Pseudo-nitzschia seriata* (Bacillariophyceae) in Scottish waters. *Journal of Phycology*, *40*(4), 622-630.

Fernandes, L. F., Hubbard, K. A., Richlen, M. L., Smith, J., Bates, S. S., Ehrman, J., Léger, C., Mafra Jr., L, Kulis, D., Quilliam, M., Libera, K., McCauley, L., & Anderson, D. M. (2014). Diversity and toxicity of the diatom *Pseudo-nitzschia* Peragallo in the Gulf of Maine, Northwestern Atlantic Ocean. *Deep Sea Research Part II: Topical Studies in Oceanography*, *103*, 139-162.

Fritz, L., Quilliam, M. A., Wright, J. L., Beale, A. M., & Work, T. M. (1992). An outbreak of domoic acid poisoning attributed to the pennate diatom *Pseudo-nitzschia australis*. *Journal of Phycology*, *28*(4), 439-442.

Fryxell, G. A., Villac, M. C., & Shapiro, L. P. (1997). The occurrence of the toxic diatom genus *Pseudo-nitzschia* (Bacillariophyceae) on the West Coast of the USA, 1920–1996: a review. *Phycologia*, *36*(6), 419-437.

García-Corona, J. L., Hégaret, H., Deléglise, M., Marzari, A., Rodríguez-Jaramillo, C., Foulon, V., & Fabioux, C. (2022). First subcellular localization of the amnesic shellfish toxin, domoic acid, in bivalve tissues: Deciphering the physiological mechanisms involved in its long-retention in the king scallop *Pecten maximus*. *Harmful Algae*, *116*, 102251.

Giffin, D., & Corbett, D. R. (2003). Evaluation of sediment dynamics in coastal systems via short-lived radioisotopes. *Journal of Marine Systems*, *42*(3-4), 83-96.

Gobler, C. J. (2020). Climate change and harmful algal blooms: insights and perspective. *Harmful algae*, *91*, 101731.

Gran, H. H. (1933). Studies on the biology and chemistry of the Gulf of Maine: II. Distribution of phytoplankton in August, 1932. *The Biological Bulletin*, *64*(2), 159-182.

Grover, J. P. (1990). Resource competition in a variable environment: phytoplankton growing according to Monod's model. *The American Naturalist*, *136*(6), 771-789.

Hallegraeff, G. M., Steffensen, D. A., & Wetherbee, R. (1988). Three estuarine Australian dinoflagellates that can produce paralytic shellfish toxins. *Journal of Plankton Research*, *10*(3), 533-541.

Hallegraeff, G. M., Bolch, C. J., Bryan, J., & Koerbin, B. (1990). Microalgal spores in ship's ballast water: a danger to aquaculture. In *4th International Conference on Toxic Marine Phytoplankton* (pp. 475-480).

Hallegraeff, G., & Gollasch, S. (2006). Anthropogenic introductions of microalgae. *Ecology of Harmful Algae*, 379-390.

Hallegraeff, G., Enevoldsen, H., & Zingone, A. (2021). Global harmful algal bloom status reporting. *Harmful Algae*, *102*, 101992.

Hansen, L. R., í Soylu, S., Kotaki, Y., Moestrup, Ø., & Lundholm, N. (2011). Toxin production and temperature-induced morphological variation of the diatom *Pseudo-nitzschia seriata* from the Arctic. *Harmful Algae*, *10*(6), 689-696.

Hasle, G. R. (1965). *Nitzschia* and *Fragilariopsis* species studied in the light and electron microscopes. II. The group *Pseudo-nitzschia*. *Skr. Norske Vidensk-Akad. I. Mat.-Nat. Kl. Ny Serie*, *18*, 1-45.

Hasle, G. R., & Lundholm, N. (2005). *Pseudo-nitzschia seriata* f. *obtusa* (Bacillariophyceae) raised in rank based on morphological, phylogenetic and distributional data. *Phycologia*, *44*(6), 608-619.

Hasle, G. R., Lange, C. B., & Syvertsen, E. E. (1996). A review of *Pseudo-nitzschia*, with special reference to the Skagerrak, North Atlantic, and adjacent waters. *Helgoländer Meeresuntersuchungen*, *50*(2), 131-175.

Hernández-Becerril, D. U. (1998). Species of the planktonic diatom genus *Pseudo-nitzschia* of the Pacific coasts of Mexico. Hydrobiologia, 379(1-3), 77-84.

Hillebrand, H., & Sommer, U. (1996). Nitrogenous nutrition of the potentially toxic diatom *Pseudo-nitzschia pungens* f. *multiseries* Hasle. *Journal of Plankton Research*, *18*(2), 295-301.

Huang, C. X., Dong, H. C., Lundholm, N., Teng, S. T., Zheng, G. C., Tan, Z. J., Lim, P. T., & Li, Y. (2019). Species composition and toxicity of the genus *Pseudo-nitzschia* in Taiwan Strait, including *P. chiniana* sp. nov. and *P. qiana* sp. nov. *Harmful Algae*, *84*, 195-209.

Hubbard, K. A., Olson, C. E., & Armbrust, E. V. (2014). Molecular characterization of *Pseudo-nitzschia* community structure and species ecology in a hydrographically complex estuarine system (Puget Sound, Washington, USA). *Marine Ecology Progress Series*, *507*, 39-55.

Hubbard, K. A., Rocap, G., & Armbrust, E. V. (2008). Inter-and intraspecific community structure within the diatom genus *Pseudo-nitzschia* (Bacillariophyceae). *Journal of Phycology*, *44*(3), 637-649.

Hubbard, K., Anderson, D., Archer, S., Berger, H., Brosnahan, M., Chadwick, C., Denny, E., Disney, J., Farrell, A., Granholm, A., Fleiger, J., Flewelling, L., Heil, C., Henschen, K., Kanwit, K., Kulis, D., Keafer, B., Keller Abbe, S., Lewis, B., Markley, L., Park, J., Petitpas, C., Racicot, E., Robert, M., Villac, C., McGillicuddy, D., 2017. Synergistic characterization of *Pseudo-nitzschia* communities during unprecedented domoic acid events. In: *Ninth Symposium on Harmful Algae in the U.S. Baltimore, MD*. pp. 135.

Kaczmarska, I., LeGresley, M. M., Martin, J. L., & Ehrman, J. (2005). Diversity of the diatom genus *Pseudo-nitzschia* Peragallo in the Quoddy Region of the Bay of Fundy, Canada. *Harmful Algae*, *4*(1), 1-19.

Kaczmarska, I., Reid, C., Martin, J. L., & Moniz, M. B. (2008). Morphological, biological, and molecular characteristics of the diatom *Pseudo-nitzschia delicatissima* from the Canadian Maritimes. *Botany*, *86*(7), 763-772.

Kudela, R. M., Cochlan, W. P., & Dugdale, R. C. (1997). Carbon and nitrogen uptake response to light by phytoplankton during an upwelling event. *Journal of Plankton Research*, *19*(5), 609-630.

Lange, C. B., Reid, F. M. H., & Vernet, M. (1994). Temporal distribution of the potentially toxic diatom *Pseudo-nitzschia australis* at a coastal site in Southern California. *Marine Ecology Progress Series*, 309-312.

Leandro, L. F., Rolland, R. M., Roth, P. B., Lundholm, N., Wang, Z., & Doucette, G. J. (2010). Exposure of the North Atlantic right whale *Eubalaena glacialis* to the marine algal biotoxin, domoic acid. *Marine Ecology Progress Series*, *398*, 287-303.

Lefebvre, K. A., Bargu, S., Kieckhefer, T., & Silver, M. W. (2002). From sanddabs to blue whales: the pervasiveness of domoic acid. *Toxicon*, *40*(7), 971-977.

Lefebvre, K. A., Powell, C. L., Busman, M., Doucette, G. J., Moeller, P. D., Silver, J. B., Miller, P. E.., Hughes, M. P., Singaram, S., Silver, M. W., & Tjeerdema, R. S. (1999). Detection of domoic acid in northern anchovies and California sea lions associated with an unusual mortality event. *Natural Toxins*, *7*(3), 85-92.

Lelong, A., Hégaret, H., Soudant, P., & Bates, S. S. (2012). *Pseudo-nitzschia* (Bacillariophyceae) species, domoic acid and amnesic shellfish poisoning: revisiting previous paradigms. *Phycologia*, *51*(2), 168-216.

Lewis, N. I., Bates, S. S., McLachlan, J. L., & Smith, J. C. (1993). Temperature effects on growth, domoic acid production, and morphology of the diatom *Nitzschia pungens* f. *multiseries*. *Toxic Phytoplankton Blooms in the Sea*, 601-606.

Li, W. K. W. (2002). Macroecological patterns of phytoplankton in the northwestern North Atlantic Ocean. *Nature*, *419*(6903), 154-157.

Li, Y., He, R., & McGillicuddy Jr, D. J. (2014). Seasonal and interannual variability in Gulf of Maine hydrodynamics: 2002–2011. *Deep Sea Research Part II: Topical Studies in Oceanography*, *103*, 210-222.

Liefer, J. D., MacIntyre, H. L., Novoveská, L., Smith, W. L., & Dorsey, C. P. (2009). Temporal and spatial variability in *Pseudo-nitzschia* spp. in Alabama coastal waters: a "hot spot" linked to submarine groundwater discharge? *Harmful Algae*, *8*(5), 706-714.

Litchman, E., Klausmeier, C. A., Schofield, O. M., & Falkowski, P. G. (2007). The role of functional traits and trade-offs in structuring phytoplankton communities: scaling from cellular to ecosystem level. *Ecology Letters*, *10*(12), 1170-1181.

Lopez, C. B., Tilney, C. L., Muhlbach, E., Bouchard, J. N., Villac, M. C., Henschen, K. L., Markley, L. R., Keller Abbe, S., Shankar, S., Shea, C. P., Flewelling, L., Garrett, M., Badylak, S., Phlips, E. J., Hall, L. M., Lasi, M. A., Parks, A. A., Paperno, R., Adams, D. H., Edwards, D. D., Schneider, J. E., Wald, K. B., Biddle, A. R., Landers, S. L., & Hubbard, K. A. (2021). High-resolution spatiotemporal dynamics of harmful algae in the Indian River Lagoon (Florida)—A case study of *Aureoumbra lagunensis*, *Pyrodinium bahamense*, and *Pseudo-nitzschia*. *Frontiers in Marine Science*, *8*, 769877.

Lundholm, N., Skov, J., Pocklington, R., & Moestrup, Ø. (1997). Studies on the marine planktonic diatom *Pseudo-nitzschia*. 2. Autecology of *P. pseudodelicatissima* based on isolates from Danish coastal waters. *Phycologia*, *36*(5), 381-388.

Lundholm, N., Hasle, G. R., Fryxell, G. A., & Hargraves, P. E. (2002). Morphology, phylogeny and taxonomy of species within the *Pseudo-nitzschia americana* complex (Bacillariophyceae) with descriptions of two new species, *Pseudo-nitzschia brasiliana* and *Pseudo-nitzschia linea*. *Phycologia*, *41*(5), 480-497.

Lundholm, N., Moestrup, Ø., Hasle, G. R., & Hoef-Emden, K. (2003). A study of the *Pseudo-nitzschia pseudodelicatissima/cuspidata* complex (Bacillariophyceae): what is *P. Pseudodelicatissima*? 1. *Journal of Phycology*, *39*(4), 797-813.

Lundholm, N., Clarke, A., & Ellegaard, M. (2010). A 100-year record of changing *Pseudo-nitzschia* species in a sill-fjord in Denmark related to nitrogen loading and temperature. *Harmful Algae*, *9*(5), 449-457.

Lundholm, N., Krock, B., John, U., Skov, J., Cheng, J., Pančić, M., Wohlrab S., Rigby, K., Gissel Nielsen, T., Selander, E., & Harðardóttir, S. (2018). Induction of domoic acid production in diatoms—Types of grazers and diatoms are important. *Harmful Algae, 79*, 64-73.

MacIntyre, H. L., Stutes, A. L., Smith, W. L., Dorsey, C. P., Abraham, A., & Dickey, R. W. (2011). Environmental correlates of community composition and toxicity during a bloom of *Pseudo-nitzschia* spp. in the northern Gulf of Mexico. *Journal of Plankton Research*, *33*(2), 273-295.

Marchetti, A., Trainer, V. L., & Harrison, P. J. (2004). Environmental conditions and phytoplankton dynamics associated with *Pseudo-nitzschia* abundance and domoic acid in the Juan de Fuca eddy. *Marine Ecology Progress Series*, *281*, 1-12.

Marshall, HG.; Cohn, MS. NOAA Technical memorandum NMFS-F/NEC-8. National Marine Fisheries Service; Woods Hole, MA. (1981). Phytoplankton community structure in northeastern coastal waters of the United States for October 1978; p. 1-49.

McCabe, R. M., Hickey, B. M., Kudela, R. M., Lefebvre, K. A., Adams, N. G., Bill, B. D., Gulland, F. M. D., Thomson, R. E., Cochlan, W. P., & Trainer, V. L. (2016). An unprecedented coastwide toxic algal bloom linked to anomalous ocean conditions. *Geophysical Research Letters*, *43*(19), 10-366.

Miller, R. L., & Kamykowski, D. L. (1986). Effects of temperature, salinity, irradiance and diurnal periodicity on growth and photosynthesis in the diatom *Nitzschia americana*; light-saturated growth. *Journal of Phycology*, *22*(3), 339-348.

Miller, P. E., & Scholin, C. A. (1996). Identification of cultured *Pseudo-nitzschia* (Bacillariophyceae) using species-specific LSU rRNA-targeted fluorescent probes. *Journal of Phycology*, *32*(4), 646-655.

Moore, S. K., Cline, M. R., Blair, K., Klinger, T., Varney, A., & Norman, K. (2019). An index of fisheries closures due to harmful algal blooms and a framework for identifying vulnerable fishing communities on the US West Coast. *Marine Policy, 110*, 103543.

Orsini, L., Procaccini, G., Sarno, D., & Montresor, M. (2004). Multiple rDNA ITS-types within the diatom *Pseudo-nitzschia delicatissima* (Bacillariophyceae) and their relative abundances across a spring bloom in the Gulf of Naples. *Marine Ecology Progress Series*, *271*, 87-98.

Pan, Y., Bates, S. S., & Cembella, A. D. (1998). Environmental stress and domoic acid production by *Pseudo-nitzschia*: a physiological perspective. *Natural Toxins*, *6*(3-4), 127-135.

Pan, Y., DV, S. R., Mann, K. H., Brown, R. G., & Pocklington, R. (1996a). Effects of silicate limitation on production of domoic acid, a neurotoxin, by the diatom *Pseudo-nitzschia multiseries*. I. Batch culture studies. *Marine Ecology Progress Series*, *131*, 225-233.

Pan, Y., Subba Rao, D. V., & Mann, K. H. (1996b). Changes in domoic acid production and cellular chemical composition of the toxigenic diatom *Pseudo-nitzschia multiseries* under phosphate limitation. *Journal of Phycology*, *32*(3), 371-381.

Parsons, M. L., & Dortch, Q. (2002). Sedimentological evidence of an increase in *Pseudo-nitzschia* (Bacillariophyceae) abundance in response to coastal eutrophication. *Limnology and Oceanography*, *47*(2), 551-558.

Percopo, I., Ruggiero, M. V., Sarno, D., Longobardi, L., Rossi, R., Piredda, R., & Zingone, A. (2022). Phenological segregation suggests speciation by time in the planktonic diatom *Pseudo-nitzschia allochrona* sp. nov. *Ecology and Evolution*, *12*(8), e9155.

Perl, T. M., Bédard, L., Kosatsky, T., Hockin, J. C., Todd, E. C., & Remis, R. S. (1990). An outbreak of toxic encephalopathy caused by eating mussels contaminated with domoic acid. *New England Journal of Medicine*, *322*(25), 1775-1780.

Pershing, A. J., Mills, K. E., Dayton, A. M., Franklin, B. S., & Kennedy, B. T. (2018). Evidence for adaptation from the 2016 marine heatwave in the Northwest Atlantic Ocean. *Oceanography*, *31*(2), 152-161.

Pettigrew, N. R., Townsend, D. W., Xue, H., Wallinga, J. P., Brickley, P. J., & Hetland, R. D. (1998). Observations of the Eastern Maine Coastal Current and its offshore extensions in 1994. *Journal of Geophysical Research: Oceans*, *103*(C13), 30623-30639.

Pettigrew, N. R., Churchill, J. H., Janzen, C. D., Mangum, L. J., Signell, R. P., Thomas, A. C., Townsend, D. W., Wallinga, J. P., & Xue, H. (2005). The kinematic and hydrographic structure of the Gulf of Maine Coastal Current. *Deep Sea Research Part II: Topical Studies in Oceanography*, *52*(19-21), 2369-2391.

Prince, E. K., Irmer, F., & Pohnert, G. (2013). Domoic acid improves the competitive ability of *Pseudo-nitzschia delicatissima* against the diatom *Skeletonema marinoi*. *Marine Drugs*, *11*(7), 2398-2412.

Quijano-Scheggia, S. I., Garcés, E., Lundholm, N., Moestrup, Ø., Andree, K., & Camp, J. (2009). Morphology, physiology, molecular phylogeny and sexual compatibility of the cryptic *Pseudo-nitzschia delicatissima* complex (Bacillariophyta), including the description of *P. arenysensis* sp. nov. *Phycologia*, *48*(6), 492-509.

Ramsdell, J. S., & Gulland, F. M. (2014). Domoic acid epileptic disease. *Marine Drugs*, *12*(3), 1185-1207.

Rothenberger, M. B., Burkholder, J. M., & Wentworth, T. R. (2009). Use of long-term data and multivariate ordination techniques to identify environmental factors governing estuarine phytoplankton species dynamics. *Limnology and Oceanography*, *54*(6), 2107-2127.

Rudek, J., Paerl, H. W., Mallin, M. A., & Bates, P. W. (1991). Seasonal and hydrological control of phytoplankton nutrient limitation in the lower Neuse River Estuary, North Carolina. *Marine Ecology Progress Series. 75*(2), 133-142.

Sarkar, S. K. (2018). *Marine Algal Bloom: Characteristics, Causes and Climate Change Impacts* (Vol. 4). Berlin/Heidelberg, Germany: Springer.

Sauvey, A., Claquin, P., Le Roy, B., Jolly, O., & Fauchot, J. (2023). Physiological conditions favorable to domoic acid production by three *Pseudo-nitzschia* species. *Journal of Experimental Marine Biology and Ecology*, *559*, 151851.

Scholin, C. A., Herzog, M., Sogin, M., & Anderson, D. M. (1994). Identification of group-and strain-specific genetic markers for globally distributed *Alexandrium* (Dinophyceae). II. sequence analysis of a fragment of the LSU rRNA gene. *Journal of Phycology*, *30*(6), 999-1011.

Scholin, C. A., Gulland, F., Doucette, G. J., Benson, S., Busman, M., Chavez, F. P., Cordaro, J., DeLong, R., De Vogelaere, A., Harvey, J., Haulena, M., Lefebvre, K., Lipscomb, T., Loscutoff, S., Lowenstine, L. J., Marin, R., Miller, P. E., McLellan, W. A., Moeller, P. D. R., Powell, C. L., Rowles, T., Silvangi, P., Silver, M., Spraker, T., Trainer, V., & Van Dolah, F. M. (2000). Mortality of sea lions along the central California coast linked to a toxic diatom bloom. *Nature*, *403*(6765), 80-84.

Smith, J., Gellene, A. G., Hubbard, K. A., Bowers, H. A., Kudela, R. M., Hayashi, K., & Caron, D. A. (2018). *Pseudo-nitzschia* species composition varies concurrently with domoic acid concentrations during two different bloom events in the Southern California Bight. *Journal of Plankton Research*, *40*(1), 29-45.

Sommer, U. (1994). Are marine diatoms favoured by high Si: N ratios?. *Marine Ecology Progress Series*, *115*, 309-315.

Sterling, A. R., Kirk, R. D., Bertin, M. J., Rynearson, T. A., Borkman, D. G., Caponi, M. C., Carney, J., Hubbard, K. A., King, M. A., Maranda, L., McDermith, E. J., Santos, N. R., Strock, J. P., Tully, E. M., Vaverka, S. B, Wilson, P. D., & Jenkins, B. D. (2022). Emerging harmful algal blooms caused by distinct seasonal assemblages of a toxic diatom. *Limnology and Oceanography*.

Sullivan, C. W., & Volcani, B. E. (1973). Role of silicon in diatom metabolism III. The effects of silicic acid on DNA polymerase, TMP kinase and DNA synthesis in *Cylindrotheca fusiformis*. *Biochimica et Biophysica Acta (BBA)-Nucleic Acids and Protein Synthesis*, *308*(2), 212-229.

Sullivan, C.W., Volcani, B.E. (1981). Silicon in the cell metabolism of diatoms. *Silicon and Siliceous Structures in Biological Systems*. New York: Springer-Verlag, 15– 42.

Teitelbaum, J. S., Zatorre, R. J., Carpenter, S., Gendron, D., Evans, A. C., Gjedde, A., & Cashman, N. R. (1990). Neurologic sequelae of domoic acid intoxication due to the ingestion of contaminated mussels. *New England Journal of Medicine*, *322*(25), 1781-1787.

Thessen, A. E., Dortch, Q., Parsons, M. L., & Morrison, W. (2005). Effect of salinity on *Pseudo-nitzschia* species (Bacillariophyceae) growth and distribution. *Journal of Phycology*, *41*(1), 21-29.

Thorel, M., Fauchot, J., Morelle, J., Raimbault, V., Le Roy, B., Miossec, C., Kientz-Bouchart, V., & Claquin, P. (2014). Interactive effects of irradiance and temperature on growth and domoic acid production of the toxic diatom *Pseudo-nitzschia australis* (Bacillariophyceae). *Harmful Algae*, *39*, 232-241.

Thorel, M., Claquin, P., Schapira, M., Le Gendre, R., Riou, P., Goux, D., Le Roy, B., Raimbault, V., Deton-Cabanillas, A., Bazin, P., Kientz-Bouchart, V., & Fauchot, J. (2017). Nutrient ratios influence variability in *Pseudo-nitzschia* species diversity and particulate domoic acid production in the Bay of Seine (France). *Harmful Algae*, *68*, 192-205.

Todd, E. C. (1993). Domoic acid and amnesic shellfish poisoning-a review. *Journal of Food Protection*, *56*(1), 69-83.

Townsend, D. W., Pettigrew, N. R., Thomas, M. A., Neary, M. G., McGillicuddy, D. J., & O'Donnell, J. (2015). Water masses and nutrient sources to the Gulf of Maine. *Journal of Marine Research*, *73*(3-4), 93-122.

Trainer, V. L., Hickey, B. M., & Bates, S. S. (2008). Toxic diatoms. *Oceans and Human Health: Risks and Remedies From the Sea*, *14*, 219-237.

Trainer, V. L., Bates, S. S., Lundholm, N., Thessen, A. E., Cochlan, W. P., Adams, N. G., & Trick, C. G. (2012). *Pseudo-nitzschia* physiological ecology, phylogeny, toxicity, monitoring and impacts on ecosystem health. *Harmful Algae, 14*, 271-300.

Turner, R. E., & Rabalais, N. N. (1991). Changes in Mississippi River water quality this century. *BioScience, 41*(3), 140-147.

Van Meerssche, E., & Pinckney, J. L. (2017). The influence of salinity in the domoic acid effect on estuarine phytoplankton communities. *Harmful Algae, 69*, 65-74.

Villac, M. C., Roelke, D. L., Chavez, F. P., Cifuentes, L. A., & Fryxell, G. A. (1993). *Pseudo-nitzschia australis* Frenguelli and related species from the west coast of the U. S. A.: Occurrence and domoic acid production. *Journal of Shellfish Research, 12*(2), 457-465.

Walz, P. M., Garrison, D. L., Graham, W. M., Cattey, M. A., Tjeerdema, R. S., & Silver, M. W. (1994). Domoic acid-producing diatom blooms in Monterey Bay, California: 1991-1993. *Natural Toxins, 2*(5), 271-279.

Wilkerson, F. P., Lassiter, A. M., Dugdale, R. C., Marchi, A., & Hogue, V. E. (2006). The phytoplankton bloom response to wind events and upwelled nutrients during the CoOP WEST study. *Deep Sea Research Part II: Topical Studies in Oceanography, 53*(25-26), 3023-3048.

Work, T. M., Barr, B., Beale, A. M., Fritz, L., Quilliam, M. A., & Wright, J. L. (1993). Epidemiology of domoic acid poisoning in brown pelicans (*Pelecanus occidentalis)* and Brandt's cormorants (*Phalacrocorax penicillatus*) in California. *Journal of Zoo and Wildlife Medicine*, 54-62.

Wright, J. L. C., Boyd, R. K., Freitas, A. D., Falk, M., Foxall, R. A., Jamieson, W. D., Laycock, M. V., McCulloch, A. W., McInnes, A. G., Odense, P., Pathak, V. P., Quilliam, M. A., Ragan, M. A., Sim, P. G., Thibault, P., Walter, J. A., Gilgan, M., Richard, D. J. A., & Dewar, D. (1989). Identification of domoic acid, a neuroexcitatory amino acid, in toxic mussels from eastern Prince Edward Island. *Canadian Journal of Chemistry, 67*(3), 481-490.

Zhu, Z., Qu, P., Fu, F., Tennenbaum, N., Tatters, A. O., & Hutchins, D. A. (2017). Understanding the blob bloom: Warming increases toxicity and abundance of the harmful bloom diatom *Pseudo-nitzschia* in California coastal waters. *Harmful Algae, 67*, 36-43.